

Analytical and experimental analysis of the capacity of steel wire ropes subjected to forced bending

TU Delft & Allseas Engineering
Bart C. de Jong



Delft University of Technology

Analytical and experimental analysis of the capacity of steel wire ropes subjected to forced bending

by

Bart C. de Jong

Evaluation committee

Prof.ir. F.S.K. Bijlaard

Dr.ir. M.A.N. Hendriks

Ir. R. Abspoel

Dr.ir. J. Breukels

Ir. L.J.M. Houben

A thesis submitted in fulfilment for the
degree of Master of Science in Civil Engineering
from the

Faculty of Civil Engineering and Geoscience
Department of Structural Mechanics

October 2015

“A designer knows he has achieved perfection not when there is nothing left to add, but when there is nothing left to take away.”

Antoine de Saint-Exupéry

Delft University of Technology

Abstract

Faculty of Civil Engineering and Geoscience
Department of Structural Mechanics

Master of Science

by Bart C. de Jong

Wire rope is used in numerous applications such as elevators, power lines, suspension bridges, ships and the mooring of offshore structures. In many of these applications wire rope needs to be bent. Currently the Norwegian certification instance Det Norske Veritas (DNV) prescribes a capacity reduction factor for bending wire rope. It is unclear how this formula is derived or what it is based on. Therefore the main question of this thesis is:

How does the forced bending of a steel wire rope around a shackle affect the break load of the wire rope?

A secondary research question is:

How does the forced bending of a steel wire rope relate to the reduction factor for bending enforced by DNV?

These questions are answered by constructing an analytical model. In addition experiments are performed at the laboratory of the civil engineering faculty to verify this model.

The analytical model is based on the assumption that every single wire behaves as an Euler-Bernoulli beam. The reduction in capacity is dominated by the effect of individual wires being bent, similar to a bundle of loose beams being bent. Plastic deformation needs to be considered to accurately describe smaller $\frac{D}{d}$ ratios. Due to the helix structure, axial tension causes friction forces to develop between the strands and the wires. This increases the stiffness of the wire rope and leads to higher stresses and strains when the wire rope is bent. As soon as the wires start slipping the stiffness lowers drastically and any further deformation causes a much lower increase in stress and strain.

All experiments are performed on both a 14mm and a 20mm wire rope. First an experiment is carried out to verify the test set-up and obtain the break load of a straight steel wire rope. Then a second experiment is performed to find the break load of a bent wire rope under various $\frac{D}{d}$ ratios. These two tests lead to a reduction factor for bending. The analytical model shows a good fit with the experimental results. From this it can be concluded that the model developed in this thesis is a promising way to model wire rope and leads to a fairly accurate answer for the capacity reduction due to bending.

The model developed and the DNV formula show similar reduction factors. For very small $\frac{D}{d}$ ratios the model predicts a 5% lower reduction, while at bigger $\frac{D}{d}$ ratios a higher reduction factor is predicted. The experiments show a better match with the analytical model, but due to the small differences and large standard deviation a larger sample size would be necessary to confirm this.

In addition to the main question a limited investigation was done on the bending stiffness of wire rope. With some additions to the model developed for capacity reduction it was possible to model the bending stiffness. The result is a stick slip model that defines the bending stiffness as a parameter of the axial tension and the curvature, this bending stiffness rapidly declines as the wire rope is bent and wires start slipping. Although this model is not experimentally validated, the fact that the original model it is based on is fairly accurate means it is worth investigating further.

Acknowledgements

There are many people that have helped, advised or motivated me during the writing of this thesis, I would like to mention a few here. First of all I would like to thank Jeroen Breukels for giving me the opportunity to write my master thesis at Allseas Engineering, providing me with guidance and encouraging me to follow my own plans and ideas. Furthermore I would like to thank my graduation committee consisting of Frans Bijlaard, Max Hendriks and Roland Abspoel for their advice, criticism and making sure I was able to perform my experiments on time, which would not have been possible without the much appreciated help from Arjen van Rhijn and John Hermsen.

Last but not least I would like to thank my parents for their unwavering support throughout my entire studies.

Bart de Jong

Contents

Abstract	ii
Acknowledgements	iv
List of Figures	ix
List of Tables	xi
Symbols	xii
1 Introduction	1
1.1 About steel wire rope	1
1.2 Problem description and research question	3
1.3 Research scope	5
1.4 Thesis outline	5
2 Literature review	7
2.1 Wire rope modelling methods	7
2.2 General wire rope theory	8
2.2.1 Axial force	8
2.2.2 Additional wire stresses	9
2.2.3 Radial force	9
2.2.4 Reuleaux stresses	9
2.2.5 Stresses due to rope ovalization	10
2.3 Bending without friction	11
2.4 Bending with friction	12
3 Analytical model	15
3.1 Approach	15
3.2 Material properties of wire rope	16
3.3 Coulomb friction model	16
3.4 Capacity of a wire and wire rope	17
3.5 Influence of the helix structure	18
3.6 Analytical model for capacity reduction	20
3.7 Conclusions from the analytical model	25
4 Model discussion	27

4.1	Load order	27
4.1.1	The loads	27
4.1.2	The order	28
4.1.3	Bending over a shackle	28
4.1.4	Slings	29
4.1.5	Load order on material level	30
4.1.6	Conclusions from load order	31
4.2	Bending stiffness of wire rope	32
4.2.1	Analytical model for bending stiffness	32
4.2.2	Conclusion for bending stiffness	34
4.3	Influence of lay length	35
4.4	Lifetime of wire rope	36
4.4.1	Loss of lubrication	36
4.4.2	Strain ageing	37
4.4.3	Corrosion	37
4.4.4	Fatigue	37
4.4.5	Abrasice wear	38
4.5	Numerical modelling of wire rope	38
5	Experiments	40
5.1	Goal of experiments	40
5.2	Experiment I	41
5.3	Results and observations experiment I	41
5.4	Experiment II	43
5.5	Results and observations experiment II	43
5.6	Statistical analysis	45
6	Comparison between theory and experiments	48
6.1	Comparison general wire rope theory with experiments	48
6.2	Comparison of the analytical model with experiments	49
6.3	Comparison with DNV formula	49
7	Conclusion, discussion and recommendation	52
7.1	Conclusion	52
7.2	Discussion	54
7.3	Recommendation	55
A	Material properties EIPS	56
B	Set up experiment I	58
C	Set up experiment II	60
D	Matlab model	63
E	Mathematical derivation strain in wires	65

Bibliography	67
---------------------	-----------

List of Figures

1.1	Wire rope buildup	2
1.2	Regular and Lang's lay wire rope	3
1.3	Different cases of wire rope being bent	3
1.4	Reduction in wire rope capacity versus $\frac{D}{d}$ ratio according to DNV formula	4
2.1	Three main categories for wire rope models according to Spak [1]	7
2.2	Wire rope ovalization	10
2.3	Relation between curvature and moment according to Papailiou [2]	13
2.4	Friction between wires according to Papailiou [2]	14
3.1	Stress-strain diagram of EIPS	16
3.2	Plastic capacity of a wire	18
3.3	Deformation of straight wires. (a) initial conditions (b) bending of free wires (c) bending of locked wires	19
3.4	Deformation of wires in helix. (a) initial conditions (b) bending of free wires (c) bending of locked wires	20
3.5	Deformation and strains due to an axial load	21
3.6	Radial forces, only the part perpendicular to the neutral axis will generate friction forces	22
3.7	Deformation and strains while (a) sticking (b) one layer slipping (c) two layers slipping (d) all layers slipping	22
3.8	Flowchart Matlab	23
3.9	Capacity reduction versus $\frac{D}{d}$ ratio for analytical model versus DNV formula of (a) 6x36WS d=20mm (b) 6x36WS d=40mm (c) 6x19WS d=20mm (d) 6x19WS d=40mm	24
3.10	Capacity reduction versus $\frac{D}{d}$ ratio for analytical model with 50% and 95% confidence level	25
4.1	Reduction in capacity versus wire stress for the two different load orders, $\frac{D}{d}=1$ $\mu=0.15$ d=20mm	29
4.2	Wire curvature as axial load is applied	29
4.3	Different slings types	30
4.4	Construction of a sling by splicing	30
4.5	Effect of load order on material level	31
4.6	Slip order of the wires, gaps indicate slipping (a) no slip (b) strands slipping (c) outer layer of strands slipping	33
4.7	Bending stiffness [EI] versus curvature (a) 6x36WS wire rope d=20 mm (b) 6x19WS wire rope d=20 mm	34
4.8	Wire rope (a) bending length (b) lay length	35

4.9	Stress strain diagram, increase of break strength at the cost of ductility due to strain ageing	37
4.10	Effect of number of wires on abrasion and fatigue	38
5.1	100 tons Losenhausen tensile testing machine	40
5.2	Overview experiment I (a) test specimen (b) overview test set-up	41
5.3	Photographs test specimen (a) (b) (c) specimen number 4, d=14 mm (d) (e) (f) specimen number 7, d=20 mm	42
5.4	Overview experiment II (a) test specimen (b) overview test set-up	44
5.5	Photographs test specimen 9, d=20 mm $\frac{D}{d}=2$ (a) before test (b)(c) during test (d)(e)(f) after test	45
5.6	Confidence interval for reduction factor (a) d=14mm (b) d=20mm	46
6.1	Reduction factor versus $\frac{D}{d}$ ratio for confidence interval of experiments and analytical model with 50% and 95% confidence level (a) d=14mm (b) d=20mm	50
6.2	Reduction factor versus $\frac{D}{d}$ ratio for confidence interval of experiments, analytical model with 50% and 95% confidence level and DNV formula (a) d=14mm (b) d=20mm	51
A.1	Stress strain diagram from tensile test performed by Bridon for steel quality 1960 $\frac{N}{mm^2}$ loaded until break	56
A.2	Stress-strain diagram of EIPS used for modelling	57
B.1	Plates for attaching cables to tensile machine	58
B.2	Test set up experiment I	59
C.1	Plates for attaching cables to tensile machine	60
C.2	Fork used to bend cables	61
C.3	Test set up experiment II	62
D.1	Input required in Matlab	63
D.2	Geometry Matlab input explained	64
D.3	Output given by Matlab	64
E.1	Difference in strain wires between wires due to helix angle	65

List of Tables

5.1	Overview experiment I results (a) d=14 mm (b) d=20 mm	42
5.2	Overview experiment II results (a) d=14 mm (b) d=20 mm	44
5.3	P-values for analytical model with 50% confidence level	47

Symbols

A	area of a wire	mm^2
d	wire rope diameter	mm
D	diameter of the bend	mm
E	modulus of elasticity	$\frac{\text{N}}{\text{mm}^2}$
F	external axial force	N
F_{bent}	break load of a bent cable	$[\text{kN}]$
F_{straight}	break load of a straight cable	$[\text{kN}]$
I	second moment of area	mm^4
M	bending moment	Nmm
n	number of wires	—
R	capacity reduction of a bent cable	$[-]$
r	distance wire to center strand	mm
W	section modulus	mm^3
Z_i	force in a wire due to axial load	N
$Z_{i,\text{friction}}$	maximum friction force in a wire	$\frac{\text{N}}{\text{mm}^2}$
α	lay angle of the wire or strand respectively	mm
γ_b	reduction factor for bending	—
δ	wire diameter	mm
κ	curvature	mm^{-1}
σ_t	stress in a wire parallel to the wire	$\frac{\text{N}}{\text{mm}^2}$
σ_b	stresses due to bending	$\frac{\text{N}}{\text{mm}^2}$
μ	Coulomb friction coefficient	—
ϕ	angle indicating wire position within a strand cross section	—

Chapter 1

Introduction

This chapter will give a short introduction to the history, uses and build-up of steel wire rope. Followed by the problem description, research question and outline of the thesis.

1.1 About steel wire rope

Steel wire rope has been used around the world for many years in numerous applications. It was first developed for hoisting in mines around 1830 [3], but its use quickly expanded to elevators, power lines, suspension bridges, ships and the mooring of offshore structures. Historically, wire rope evolved from steel chains. Due to its build-up, steel chains suffer from critical failure in case a single member fails. Wire rope however is much more resistant to flaws or failure of a single wire and this is one of the reasons it is preferred over chains.

In the offshore industry wire rope is of great importance and frequently used for connecting various parts and lifting heavy objects. It is subject to heavy loads, often of a dynamic nature. Wire rope does not give any warning before failure while it has a critical role in a mechanical system. Because of this a high safety factor is used, sometimes being as high as 6!

For such a frequently used mechanical part the amount of theoretical models are limited and relatively recent. Cables were initially modelled as strings in tension [4] [5] [6]. This involves a negligible bending and torsion stiffness. However, the stiffness value for bending and torsion are not negligible for cables, especially when the diameter increases. A lot of effort has been put in modelling wire rope using a beam formulation. Costello [7] was one of the first to incorporate the bending and torsion stiffness of the individual

wires of a wire rope as thin rods. Here the wire rope geometry starts to play a major role.

In contrast to the thin rod model, Raoof and Hobbs [8] and Jolicoeur and Cardou [9] created semi-continuous models. Here every layer of wires is modelled as an orthotropic cylinder with properties that match those of the rope layer. Strand stiffness and inter-wire effects are taken into account.

Various finite element (FE) models of wire rope under tension are available that incorporate the non-linear behaviour of wire rope [10] [11]. The amount of models that include bending of wire rope are rather limited. The free bending of a wire rope is investigated by Giglio and Manes [12].

Much less is known about the causes of the various failure mechanisms. The different failure mechanisms itself can be found in any cable inspection manual [13], but the theoretical background on what causes these failures is much less known. Wear, nicking, plastic deformation and corrosion are all common criteria on which a wire rope might be discarded. When dynamic loads are applied, fatigue is often the limiting factor for a wire rope. Although not discussed in this report it is important to consider the fatigue life when designing a wire rope under fluctuating loads.

The geometry and structure of a wire rope play a vital role. Steel wires of several millimetres are wrapped helically around a straight wire to form a strand. Sometimes a single strand is used, but for heavy loads several strands are wrapped helically around a straight strand. Both the wires and the strands can be applied in multiple layers. Figure 1.1 gives an overview of these different components. The lay angle refers to the angle the wires or strands make with the vertical axis of the strand or the rope respectively. The direction of the lay angle can be either left or right. A regular lay rope has opposite directions for wire and strand lay angles. A Lang's lay rope has similar directions for the wire and strand angle, see also figure 1.2. The total diameter of a wire rope varies between 5 to 150 millimetres.

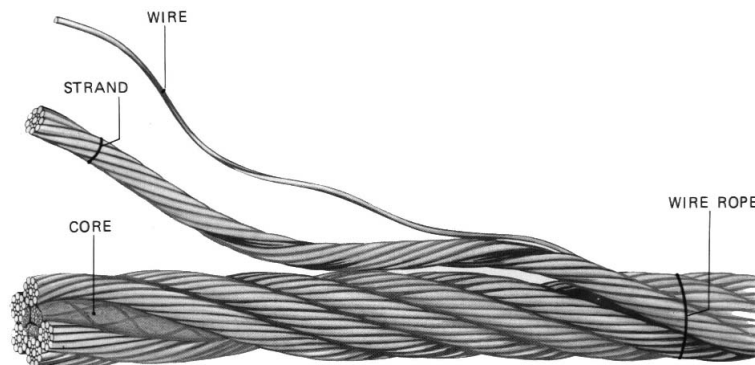


FIGURE 1.1: Wire rope buildup

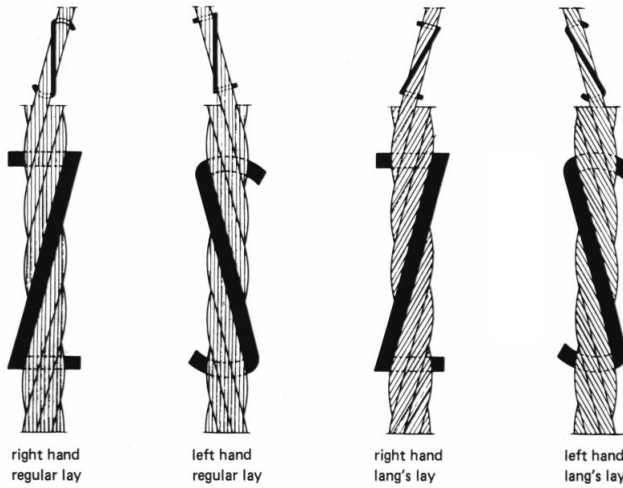


FIGURE 1.2: Regular and Lang's lay wire rope

The helix structure of the wires and the strands is an important characteristic of wire rope as will be explained in detail later. The two main reasons this helix structure is used are an increase in bending flexibility and creating bundle coherence. This does however come at the cost of axial strength and axial stiffness.

1.2 Problem description and research question

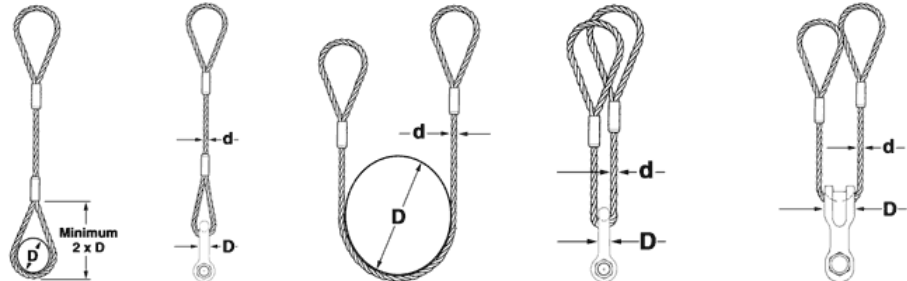


FIGURE 1.3: Different cases of wire rope being bent

When using wire rope there are many situations where the wire rope needs to be bent. Figure 1.3 shows some examples where this is the case. It seems logical that this has a big impact on the internal forces and the overall resistance of the wire rope. The most common way to calculate the reduction factor for bending wire rope is the one set-up by Det Norske Veritas (DNV). DNV is a Norwegian instance that certifies products in the energy, offshore, oil and gas industry. The current formula is [14]:

$$\gamma_b = \frac{1}{1 - \frac{0.5}{\sqrt{\frac{D}{d}}}} \quad (1.1)$$

γ_b =reduction factor for bending [-]

D =diameter of the bend [mm]

d =diameter of the wire rope [mm]

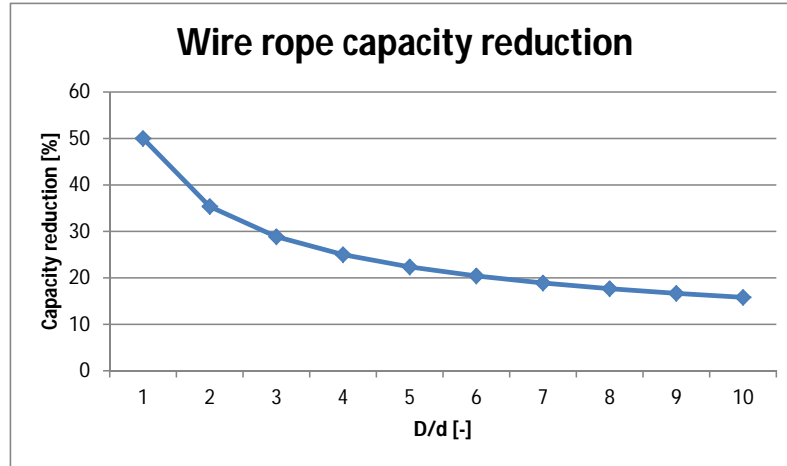


FIGURE 1.4: Reduction in wire rope capacity versus $\frac{D}{d}$ ratio according to DNV formula

Figure 1.4 shows a graph of the $\frac{D}{d}$ ratio versus the reduction in breaking strength this formula leads to. As can be seen, small $\frac{D}{d}$ ratios give a large reduction in the capacity of the wire rope. While this reduction factor is used in almost every engineering application where wire rope is bent, it is unclear how this formula is derived or what it is based on. Therefore the main research question of this paper is:

How does the forced bending of a steel wire rope around a shackle affect the break load of the wire rope?

A secondary research question is:

How does the forced bending of a steel wire rope relate to the reduction factor for bending enforced by DNV?

A few terms mentioned in the main research question require additional explanation. Forced bending means the curvature the wire rope is subject to is equal to the object it is bend around, in this case a shackle. Especially when high loads are applied this is valid, when the wire rope is loaded it will be pulled tight around the shackle. The minimum break load (MBL) of a wire rope is defined as the lowest 5th percentile of a series of destructive test. It is also acceptable to pick the lowest value of a series of three tests [14]. The formula to calculate the MBL is 1.2.

$$MBL = \frac{d^2 R_t K}{1000} \quad (1.2)$$

$MBL = \text{minimum break load}$ [kN]

$d = \text{diameter of the wire rope}$ [mm]

$R_t = \text{rope grade}$ [$\frac{N}{mm^2}$]

$K = MBL$ factor for rope class [-]

1.3 Research scope

Wire rope is a complex mechanical part and there are many different ways to construct a wire rope, combine this with different kinds of loadings and a lot of questions arise. To limit the scope of this thesis the following boundaries are set-up:

- Only steel wire ropes with a steel wire core are considered.
- Wire ropes come in many different configuration, only a 6x36 and 6x19 are considered.
- The load on the steel wire rope is defined with an axial load and a curvature equal to the shackle bow.
- Statically loaded. Fatigue or dynamic effects are not considered.
- Only regular lay rope is used.
- Bending over a shackle is considered, although this is easily translated to other applications where wire rope is bent.

1.4 Thesis outline

Below is an outline of the build-up of this thesis

- Chapter 1 serves as an introduction to the concept of steel wire rope, the uses, its geometry and the research question.
- Chapter 2 gives an overview of the most important literature used and their contributions. The knowledge obtained from this literature is used to construct an analytical model in chapter 3.
- Chapter 3 presents an analytical model that predicts the failure and capacity reduction of a bent wire rope.

- Chapter 4 discusses a number of interesting concepts discovered during the development of the analytical model. These subjects are closely related to the bending of wire rope, but did not necessarily fit in chapter 3.
- In chapter 5 the goal, results and observations of the experiments performed to validate the analytical model are discussed.
- In chapter 6 a comparison is made between the analytical model, the DNV formula and the experimental results.
- Chapter 7 present the overall conclusion, discussion and recommendation of this thesis.

Chapter 2

Literature review

Various literature has been studied while writing this thesis. In this chapter an overview is given of the most important literature. The content of this literature is used in chapter 3 to construct an analytical model for the bending of wire rope. It is also useful to obtain a general idea of how wire rope works.

2.1 Wire rope modelling methods

In Spak [1] an excellent overview of all available methods for modelling wire rope is given. The different wire rope models are divided in three categories. These categories are: thin-rod, string/beam and semi-continuous. Figure 2.1 gives an overview of these categories.

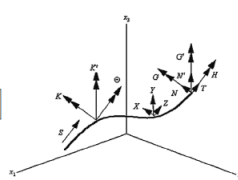
Model type	Representative governing equations	Method
Thin-rod	Based on summation of forces of a curved rod: $\begin{aligned} -N'\tau + T\kappa' + X &= 0 \\ -G'\tau + H\kappa' - N' &= 0 \end{aligned}$ <p>Stiffness matrix is developed, Cable response is calculated:</p> $[F] = \begin{bmatrix} k_{xx} & k_{x\theta} \\ k_{\theta x} & k_{\theta\theta} \end{bmatrix} \begin{bmatrix} u \\ \theta \end{bmatrix}$ 	Equilibrium equations are used to determine the loads on the wire. Curvature and twist of the cable are related to the internal loads, and force and moment equations are developed. A stiffness matrix is created based on the cable properties, and axial and torsional responses can be calculated.
String/beam	String: $m\ddot{w} - Tw'' = 0$ Euler-Bernoulli: $\rho A\ddot{w} + EIw''' - Tw'' = 0$ Shear: $\rho A\ddot{w} - KGA(w'' - \psi') = f(x, t)$ $EI\psi'' + KGA(w' - \psi) = 0$	Cables are modeled as strings (no bending stiffness) or beams, with properties developed to accurately incorporate cable bending and stiffness.
Semicontinuous	$\begin{Bmatrix} \sigma_x \\ \sigma_y \\ \sigma_z \\ \sigma_{yz} \\ \sigma_{xz} \\ \sigma_{xy} \end{Bmatrix} = [C] \begin{Bmatrix} \varepsilon_x \\ \varepsilon_y \\ \varepsilon_z \\ \gamma_{yz} \\ \gamma_{xz} \\ \gamma_{xy} \end{Bmatrix}$ <p>where $[C]$ is a matrix of elastic stiffnesses related to the cable's material properties</p>	Cables in each layer are modeled as a homogenous hollow cylinder with global properties. Then, constitutive equations for the cylinder are analyzed using various methods (i.e., stress-strain relations) to determine cable behavior.

FIGURE 2.1: Three main categories for wire rope models according to Spak [1]

In these models inter wire friction is treated in various ways, the most common ways are: no inter wire friction, only friction between different layers (not between wires in the same layer) and friction between all wires. The inclusion of friction leads to a bi-linear bending stiffness diagram. Where the bending stiffness is dependent on the curvature and the axial tension. Most models that include friction only use inter layer friction, because this plays an important role in the bending stiffness. Thin-rod models are most appropriate for modelling the friction in the wire rope.

2.2 General wire rope theory

In Feyrer [15] an extensive overview of wire rope geometry is given followed by a description of all the forces working on a wire rope under axial tension, bending and several formulas for calculating them. Due to its geometry the forces working on and inside a wire rope become more complex than one might think at first. Therefore it is better to view wire rope as a machine with many moving parts instead of a simple tension member. Below is an overview of all the forces working in a wire rope. Feyrer is based on the thin-rod model.

2.2.1 Axial force

Before looking into bending, a wire rope under pure tension is discussed. When a wire rope is first tensioned all the wires settle a bit and the wire rope suffers a large extension at a very low force. This is a highly non-linear effect and is normally eliminated by stressing the ropes before actually using them. Once the rope has settled and is brought under tension again it is the central wire that experiences the greatest strain. The wires in the single and double helix will extend less than the central wire because they are at an angle with the centroid so will have lower stresses than the central wire rope. This means that in an axial loaded wire rope the central wire is the first wire to yield and eventually fail. The axial stresses in the wires of a straight strand can be calculated according to formula 2.1.

$$\sigma_t = \frac{\cos^2 \alpha_k E_k}{\sum_i \cos^3 \alpha_i E_i A_i} F \quad (2.1)$$

For an entire wire rope the expression extends to formula 2.2.

$$\sigma_t = \frac{(\cos^2 \alpha_k \cos^2 \alpha_{kl}) E_{kl}}{\sum_i (\cos^3 \alpha_i) \sum_{ij} (\cos^3 \alpha_{ij}) E_{ij} A_{ij}} F \quad (2.2)$$

σ_t =stress in a wire parallel to the wire [$\frac{N}{mm^2}$]

α =lay angle of the wire or strand respectively [-]

F =external axial force [N]

E =modulus of elasticity [$\frac{N}{mm^2}$]

A =area of a wire [mm^2]

subscript k refers to a specific wire

subscript l refers to a specific strand

subscript i refers to all wires in a layer

subscript j refers to all strands in a wire rope

For steel wire ropes with a Poisson coefficient of 0.3 the influence of lateral contraction on the stresses in the wire is small. Giving differences in stress of 2% to 3%. For other materials, for example a fibre rope core, it can lead to bigger differences.

2.2.2 Additional wire stresses

Under tensile force the wire rope will become longer and thinner. This causes the helix to deform and introduces additional bending stresses, torsion stresses and radial pressure. These additional stresses are not very large and play a minor role when fluctuating stresses become important.

2.2.3 Radial force

The wires in the helix also exert a radial force on the central wire when the rope is tensioned. The helix shape wants to contract and this causes the wires to grip onto the central wire. These radial forces increase the potential friction forces possible between the wires (Coulomb friction). This plays a role when the wire rope is bent.

2.2.4 Reuleaux stresses

In Feyrer the classic method of calculating stresses induced by bending is discussed. This is the Reuleaux stress which is a very simple method to calculate the bending stress. It is based on loose wires lying on top of each other and does not incorporate the helix structure. With general beam theory the formula 2.3 can be derived.

$$M = \kappa EI$$

$$M = \sigma_b W$$

$$\kappa = \frac{2}{D}$$

$$\sigma_b = \frac{2}{D} \frac{I}{W} E$$

$$\sigma_b = \frac{\delta}{D} E \quad (2.3)$$

M =bending moment [Nmm]

κ =curvature [mm^{-1}]

E =modulus of elasticity [$\frac{N}{mm^2}$]

I =second moment of area [mm^4]

W =section modulus [mm^3]

D =bending diameter [mm]

δ =diameter of a wire [mm]

σ_b =stresses due to bending [$\frac{N}{mm^2}$]

Which is defined as the Reuleaux stress.

2.2.5 Stresses due to rope ovalization

The groove radius is normally greater than the rope diameter. When the rope is loaded in axial direction it will flatten a little causing the rope to adopt a more oval shape, see figure 2.2. The change in curvature the rope undergoes while transforming from a circular to a elliptical cross section causes stresses to occur. Normally the groove radius is chosen in such a way that it matches the rope diameter these stresses will be very small and in such cases can be ignored.

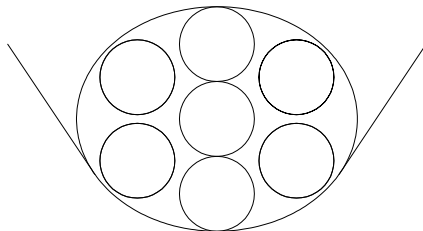


FIGURE 2.2: Wire rope ovalization

2.3 Bending without friction

The basic mechanics and mathematics of the wire rope are discussed in Theory of Wire Rope [7]. The mathematics behind the helix configuration of the wires and the strands are derived and the effect this has on the characteristics of the wire rope. This theory is based on the assumption that each individual wire behaves as a simple beam and the whole cross section functions as a bundle of independent beams. The following assumptions are made:

- Each individual wire behaves as an Euler-Bernoulli beam.
- Material behaviour is linear elastic.
- No inter wire friction.
- Change in lay angle is ignored.
- Rope ovalization is ignored.

For the central wire that is not part of the helix structure this gives the following relation:

$$M = \frac{E\pi}{64} \delta_1^4 \kappa \quad (2.4)$$

For the wires in a single helix the relation changes to:

$$M = \frac{E\pi}{64} \frac{2 \cos \alpha_1}{2 + \nu \sin^2 \alpha_1} \delta_2^4 \kappa \quad (2.5)$$

Here a factor is added that reduces the second moment of area depending on the lay angle and the Poisson ratio. The mathematical derivation of this factor is shown in appendix E. In case of a complete wire rope the wires in the outside strands are composed of a helix wrapped around another helix. For these wires the following relation is valid:

$$M = \frac{E\pi}{64} \frac{2 \cos \alpha_1}{2 + \nu \sin^2 \alpha_1} \frac{2 \cos \alpha_2}{2 + \nu \sin^2 \alpha_2} \delta_3^4 \kappa \quad (2.6)$$

For wires in a double helix the factor is added again, both with their own lay angle and corresponding Poisson ratio. The Poisson ratio is assumed to be the same for all wires. For the entire wire rope the relation can be obtained by summing equations 2.4 to 2.6 over the entire cross section. This leads to:

$$M = \frac{E\pi}{64} (i \frac{2 \cos \alpha_1}{2 + \nu \sin^2 \alpha_1} \frac{2 \cos \alpha_2}{2 + \nu \sin^2 \alpha_2} \delta_3^4 + j \frac{2 \cos \alpha_1}{2 + \nu \sin^2 \alpha_1} \delta_2^4 + \delta_1^4) \kappa \quad (2.7)$$

M =bending moment [Nmm]

κ =curvature [mm^{-1}]

E =modulus of elasticity [$\frac{\text{N}}{\text{mm}^2}$]

δ =diameter of a wire [mm]

α_1 =lay angle of wires [-]

α_2 =lay angle of strands [-]

2.4 Bending with friction

A different model is developed by Papailiou [2]. This model has a lot in common with the Costello model, except that it incorporates friction, which makes the model more complicated. The following assumptions are made:

- Each individual wire behaves as an Euler-Bernoulli beam.
- Material behaviour linear elastic.
- No contact between wires in the same layer.
- Change in lay angle is ignored.
- Rope ovalization is ignored.
- Friction behaviour is bi-linear.
- No friction after transition curvature has been reached.

In the case with unlimited friction between the wires (no slip), the whole wire rope cross section would act as a single beam. In case of no friction the cross section would act as a bundle of individual beams as explained in the theory by Costello. The truth lies somewhere in the middle. The cross section acts as a single beam until the wires start slipping. In between these zones is the transition zone, here part of the wires are slipping and the other wires are still in stick mode. This leads to a stiffness diagram as shown in figure 2.3.

Here $EI_{regionI}$ is the sum of the stiffness of the individual wires, there is however an additional stiffness part based on the interaction(friction) between the wires. The amount

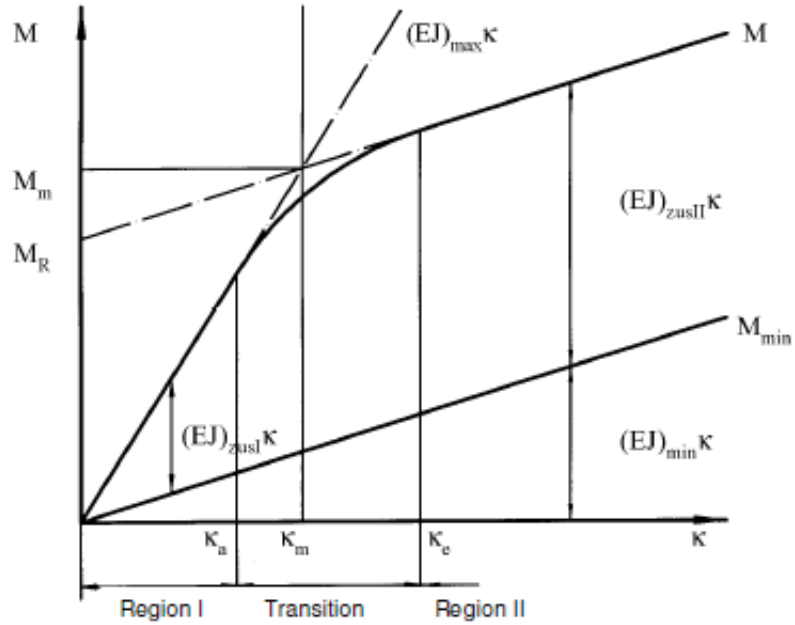


FIGURE 2.3: Relation between curvature and moment according to Papailiou [2]

of friction between the wires has a maximum value. Once this maximum is reached the total stiffness becomes equal to $EI_{regionII}$.

$$EI_{regionI} = \sum_i \frac{n}{2} EA r^2 \cos^3 \alpha \quad (2.8)$$

$$EI_{regionII} = \sum_i n E \pi \frac{\delta^4}{64} \cos \alpha \quad (2.9)$$

n =number of wires [-]

A =surface of a wire [mm^2]

r =distance wire to center strand [mm]

α =lay angle wire [-]

As can be seen in the graph there is a transition zone where region I transitions into region II. To calculate the average curvature where this happens the maximum tensile force due to friction in each wire is required 2.10. From this tensile force the moment M_r 2.11 can be calculated and from this the transition curvature κ_m 2.12.

$$Z_{i,friction} = Z_i (e^{\mu \sin \phi} - 1) \cos \alpha \quad (2.10)$$

$$M_r = \sum_i Z_{i,friction} \sin \phi r \quad (2.11)$$

$$\kappa_m = \frac{M_r}{EI_{regionI}} \quad (2.12)$$

$Z_{i,friction}$ =maximum friction force in a wire[N]

Z_i =force in a wire due to axial load [N]

μ =Coulomb friction coefficient [-]

ϕ =angle indicating wire position within a strand cross section [-]

From the formulas it can be seen that the maximum force due to friction is dependent on the axial force in the wire rope. This is further illustrated in figure 2.4, as the helix structure is tensioned it grips onto the layers beneath it creating forces in the radial direction between layers. Assuming a simple Coulomb friction model this results in friction forces between the various layers. This has a large influence on the stiffness in region I and the point of transition between region I and region II. It can also be seen that the stiffness in region I is much larger than in region II. This means that when bending a wire rope large stresses will occur until the transition curvature is reached. After this the generated stresses will be much lower.

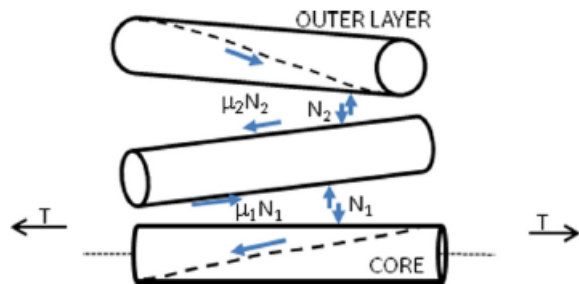


FIGURE 2.4: Friction between wires according to Papailiou [2]

When a strand consists of multiple layers there will be multiple transition points. Every layer has a certain moment or curvature where it starts to slip. This gives a moment curvature diagram with multiple kinks in it, one for every layer. With multiple layers present the radial forces increase towards the inner layers of the wire. This leads to higher friction forces between the inner layers, resulting in higher stresses in the inner wires.

Chapter 3

Analytical model

This chapter combines different theories to form a model to calculate the strains in a wire rope and give a reduction factor for axial loading. The model is programmed into a Matlab script. Before looking into the model several important concepts are discussed.

3.1 Approach

This chapter starts with the discussion of some important concepts that are needed to construct the analytical model. Below is a list of the subjects discussed in this chapter and the reason they are included.

- The steel used in wire rope is different than regular construction steel. For an accurate model reliable material properties are needed. In paragraph 3.2 the material properties of wire rope are discussed.
- In paragraph 2.4 the influence of friction is described. In paragraph 3.3 the way friction is incorporated in the model is further explained.
- Only the force distribution in a wire rope is not enough to determine the capacity reduction. Therefore in paragraph 3.4 a failure criteria and a capacity reduction for a wire and wire rope is defined.
- The geometry of a wire rope is defined by the double helix configuration. The impact this has is discussed in paragraph 3.5.
- The above mentioned concepts plus the literature discussed in chapter 2 are combined to create an analytical model that calculates the capacity loss from bending.

- Four wire ropes are modelled with this model. The results are discussed in the final paragraph.

3.2 Material properties of wire rope

Wire rope is made out of high strength steel. The most common grades of steel used for wire rope are improved plow steel (IPS), extra improved plow steel (EIPS) and extra extra improved plow steel (EEIPS). Because the wire rope will be loaded until complete failure, plasticity plays an important role. Even though high strength steel has limited deformation capacity it will allow a plastic moment to develop and to redistribute stresses over the cross section of the wire rope. In this thesis only EIPS is considered. No reliable information was available on the material properties of EIPS. To obtain the characteristics of EIPS a tension test was performed by Bridon. The results of this test are included in appendix A. The bi-linear stress-strain graph shown in figure 3.1 is based on these results.

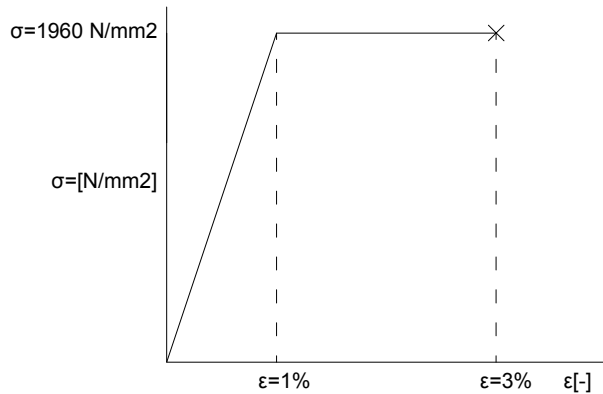


FIGURE 3.1: Stress-strain diagram of EIPS

Important parameters in figure 3.1 are

$\sigma_{yield} = 1960 \frac{N}{mm^2}$ the maximum yield stress

$\epsilon_1 = 1\%$ strain where elastic region changes into plastic region

$\epsilon_2 = 3\%$ strain where wire break occurs

3.3 Coulomb friction model

The friction is based on a Coulomb friction model. The magnitude of the friction force is dependent on the normal force F_n and the friction coefficient μ . The speed of slippage

does not play a role in this model. This leads to a stick slip friction model where the maximum amount of friction before slipping occurs is equal to equation 3.1.

$$F_w = \mu F_n \quad (3.1)$$

An important parameter in equation 3.1 is the friction coefficient μ . For steel on steel $\mu = 0.3$ is an often used value. However due to the lubrication used in wire rope much lower values should be used. Values used in papers vary from 0.115 to 0.2 [16] [17]. In [18] the friction coefficient is extensively researched and it is concluded that it is related to the normal force in the wire rope. Values for μ seem to remain close to 0.15 with some variation due to the normal force. For this model a constant value of $\mu = 0.15$ is chosen.

There was no literature found on the friction coefficient between the various strands. A friction coefficient of $\mu = 0.15$ is chosen based on the value for friction between wires. Actual values could be lower due to the lubrication used or higher because of the surface of the strand consisting of many wires, creating a ribbed, rough surface.

3.4 Capacity of a wire and wire rope

The capacity of the entire wire rope is based on the capacity of every single cross section. Imagine the wire rope is divided in numerous thin slices, if any one of these slices fail the wire rope fails. The capacity of these cross sections is based on the capacity of the wires. However, simply taking the highest capacity reduction out of all the wires and applying this to the entire rope would lead to a higher reduction than necessary. For this reason the reduction in the central wires of the strands is not taken into account. These wires are at none or a single helix angle with the centroid of the rope and this makes these wires have a significant higher reduction factor than the other wires. These wires make up roughly 5% of the entire rope cross sectional area. Under maximum load these wires will fail before other wires, but because they make up such a low percentage of the entire cross section it is assumed the load will be able to redistribute over adjacent wires.

To determine what normal force a wire can absorb before it fails the plastic deformation capacity plays an important role. Wires will fail once a plastic strain of 3% is reached at some point in the cross section of the wire. By applying Hook's law the strain in the entire cross section of a wire can be obtained. The maximum total strain in the wires is the sum of the strain from bending, friction plus any axial strain. The maximum normal

force that can develop in a wire can be calculated according to formula 3.2. This is done by integrating the surface of a wire that has not reached the yield stress multiplied with the possible extension this can undergo before it reaches the yield limit over the height of the wire. This is the maximum normal force that can develop in a wire. Comparing this with the capacity of the full cross section of a wire gives the reduction in capacity.

$$N = \int_{-0.5\delta}^{yieldheight} width_{elastic} \epsilon_{elastic} E dh \quad (3.2)$$

δ =wire diameter [mm]

$width_{elastic}$ =width of the wire in elastic region [mm] see figure 3.2

$\epsilon_{elastic}$ =amount of elastic deformation possible [-] see figure 3.2

E =modulus of elasticity [$\frac{N}{mm^2}$]

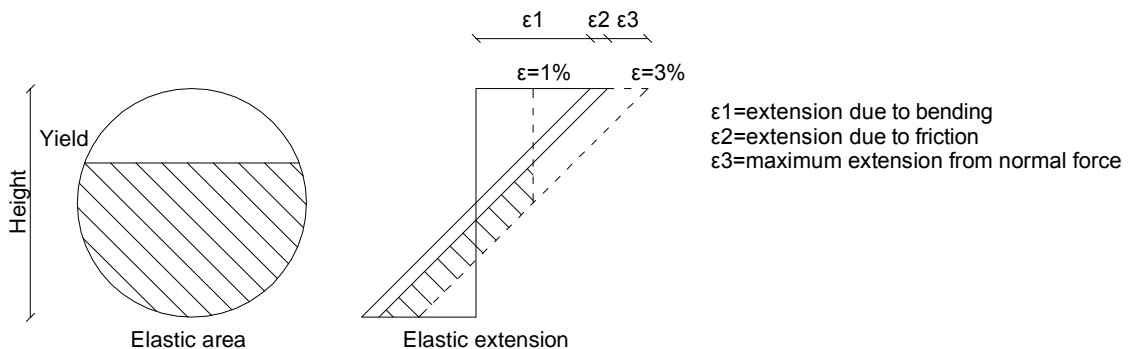


FIGURE 3.2: Plastic capacity of a wire

3.5 Influence of the helix structure

As mentioned before the helix structure plays an important role. In chapter 1 the positive and negative effects of the helix are shortly mentioned, namely:

- Loss in axial strength.
- Loss in axial stiffness.
- Bundle coherence.
- Increase in bending flexibility.

The first two effects are always unwanted, since the main function of wire rope is carrying loads in tension. The loss depends on the lay angle. A non uniform stress distribution over the cross section of the cable is the result. This effect is shown in figure 3.5. The difference in stress in the wires is dependent on the lay angle, which should be small.

The third item, bundle coherence, makes sure all the wires are being held together. In case the wires would not be held together the wires of the cable would become unstable quickly leading to failure of the wire rope.

The last item is an increase in bending flexibility. It should be noted that in most cases it is desirable to have a low bending stiffness, it is a cable after all, but in some cases it can have a negative effect. For example the forming of loops in a wire rope is resisted by a high bending stiffness. To investigate the effect of the helix structure, a wire rope with and without a helix structure is considered. In both cases it is assumed there is no friction between the wires. Figure 3.3(a) shows straight wires lying on top of each other with no load applied. In 3.3(b) a bending moment is applied, because the wires are not connected in any way they will each bend around their own neutral axis. In figure 3.3(c) the same wires are now connected at both ends. If a moment is applied the wires will bend around the neutral axis of all wires combined. The wire at the top of the cross section will have to extend, while the wires at the bottom are being compressed. This causes high axial forces in the wires and results in the cross section with the locked up wires having a much larger bending stiffness.

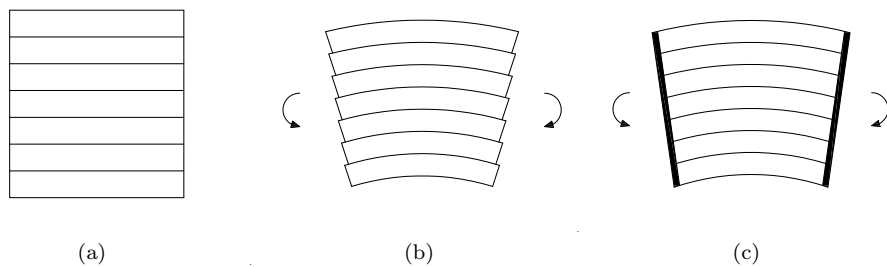


FIGURE 3.3: Deformation of straight wires. (a) initial conditions (b) bending of free wires (c) bending of locked wires

Now we will take a look at the same wires, except in a helix structure instead of parallel to each other. Figure 3.4(a) shows the initial configuration. Now when a bending moment is applied to the loose wires 3.4(b) all wires will bend around their own axis, same as in the straight case. When the locked up wires are bent 3.4(c) it can be seen that the wires will not undergo any axial deformation, because each wire is located equally in both the tension and compression side of the cross section. Each wire still has to absorb a moment around its own neutral axis. This is the same as the wires that were not locked at the ends.

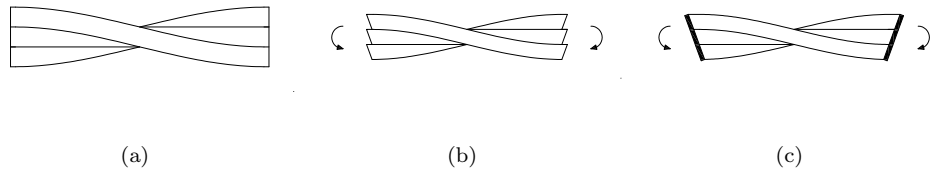


FIGURE 3.4: Deformation of wires in helix. (a) initial conditions (b) bending of free wires (c) bending of locked wires

For our model this means that when the wire rope becomes bent it will always respond with the wires bending around their individual neutral axis. Even if the wire rope is locked at the end by sockets. This leads to a much lower stiffness than a structure without a helix and is very beneficial for the stresses in the wires. A downside is the introduction of friction forces caused by the helix being tensioned as will be explained later. Overall the helix structure is very beneficial when the wire rope is bent.

3.6 Analytical model for capacity reduction

With the knowledge from the literature in chapter 2 and the above discussed concepts an analytical model is developed. To model the wire rope a thin rod model has been chosen, based on a combination of Costello, Papailiou and extended by the author of this thesis. The reason this is chosen is because thin rod models are well suited for analytical modelling. It is possible to describe the friction between the wires for each wire. This gives good insight in how the wire rope functions and allows to predict failure of individual wires. To model the plastic behaviour properly and because the bending radius is given (not the bending moment) a strain based model is chosen. The following assumptions are made in this model:

- Each individual wire behaves as an Euler-Bernoulli beam. This is the basis of thin rod models.
- Material behaviour is bi-linear with some plastic deformation. To model the failure of a wire accurately plastic deformation needs to be taken into account.
- No contact between wires in the same layer. If the diameter of the wires decreases towards the outer layers this assumption is justified, every wire rope is constructed like this.
- Rope ovalization is ignored. If the radius of the shackle matches the diameter of the rope, rope ovalisation will not have a large influence.

- Change in lay angle is ignored. According to Feyrer [15] the effect the change in lay angle has on the bending stresses is very small.
- Friction behaviour bi-linear according to Papailiou.
- No friction after transition curvature has been reached.
- Stresses occurring in the stick phase (these are the stresses from friction calculated according to Papailiou) are assumed to be constant over the cross section of a wire. In reality they would vary linearly over the height of the wire. Because the diameter of a wire is small this simplification is justified.
- Stresses occurring from the slipping and sticking of entire strands are assumed to be constant over the entire strand. This is not entirely accurate and will predict a slightly lower failure force than a varying stress.

A clear distinction should be made between the force distribution between region I, the transition zone and region II. In region I the wire rope acts as a solid cross section until the maximum friction force has been reached. Once this curvature has been reached a layer begins to slip and it will bend around its own neutral axis. Once all layers are in slip mode region II begins and the cable has reached its lowest possible stiffness. Following is a description of all the stages the wire rope goes through when tensioned and subsequently bent. At first the rope is tensioned in axial direction. This causes strains to occur in the wires. This strain differs from layer to layer because of the different helix angle the layers have. This strain distribution due to axial load is shown in figure 3.5.

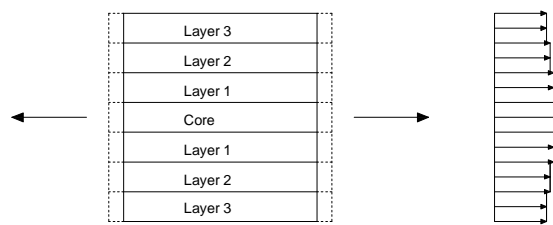


FIGURE 3.5: Deformation and strains due to an axial load

Besides the axial strains, tensioning the wire rope also causes radial forces. When the helix structure is tensioned it grips onto the layers beneath it. The radial forces increase cumulatively when multiple layers are present, because a layer pressures every layer beneath it. In case the wire rope is bent, these friction forces will at first prevent the layers from moving relatively to each other. It is important to note that when the wire rope is bent around the neutral axis, only radial forces working perpendicular to the neutral axis will generate friction forces. This concept is further explained in figure 3.6.

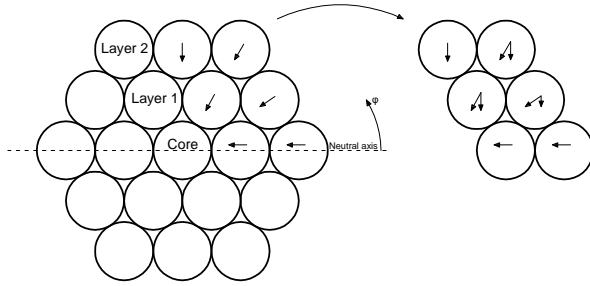


FIGURE 3.6: Radial forces, only the part perpendicular to the neutral axis will generate friction forces

When the wire rope is bent around the neutral axis strains will occur. At first the entire cross section will act as a solid beam, this is noted as region I, see 3.7(a). At a certain bending moment wires start slipping, see 3.7(b). The first wires to start slipping are the ones located in the outer layer around the neutral axis. This is because friction forces in the outer layer are the lowest and are at a small angle ϕ with the neutral axis, thus having a small vertical component. Every wire will start slipping once a certain curvature and accompanying wire force has been reached. It should be noted that these strains remain in the wire even after the wire starts slipping!

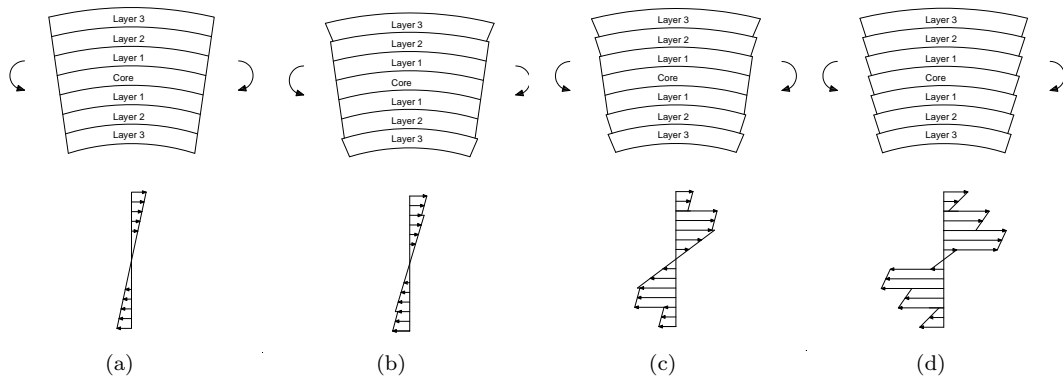


FIGURE 3.7: Deformation and strains while (a) sticking (b) one layer slipping (c) two layers slipping (d) all layers slipping

When a wire begins to slip and the curvature of the wire rope is further increased it will start bending around its own neutral axis. In the transition zone part of the wires are still sticking and others are slipping. When all the wires have started slipping the wire rope has reached its lowest stiffness and any curvature applied is absorbed by wires bending around their individual neutral axis, this is noted as region II, see 3.7(d).

Every wire in the strand now has a uniform strain from axial tension, a uniform strain from the stick phase and a varying strain from bending around its own neutral axis from

the slipping phase. Combining these strains and applying the failure criteria 3.2 defines if a wire has failed or how much capacity it has left.

Now that a separate strand has been modelled, an entire wire rope is considered. The interaction of the strands of the wire rope is modelled in a similar way as the wires of a strand are modelled. At first the wire rope is bent as a whole, after a certain curvature the strands start slipping. This introduces an extra uniform strain in the strands, depending on the friction between the strands. This extra strain is added to the strain in the strand caused by only the axial load. Furthermore the lay angle of the strands is taken into account. This is done exactly the same as for the wires, except now it reduces the axial and bending stiffness of the strands. This whole process is summarized in the flow scheme shown in figure 3.8. In appendix D a detailed explanation of the input and output in the Matlab script is provided.

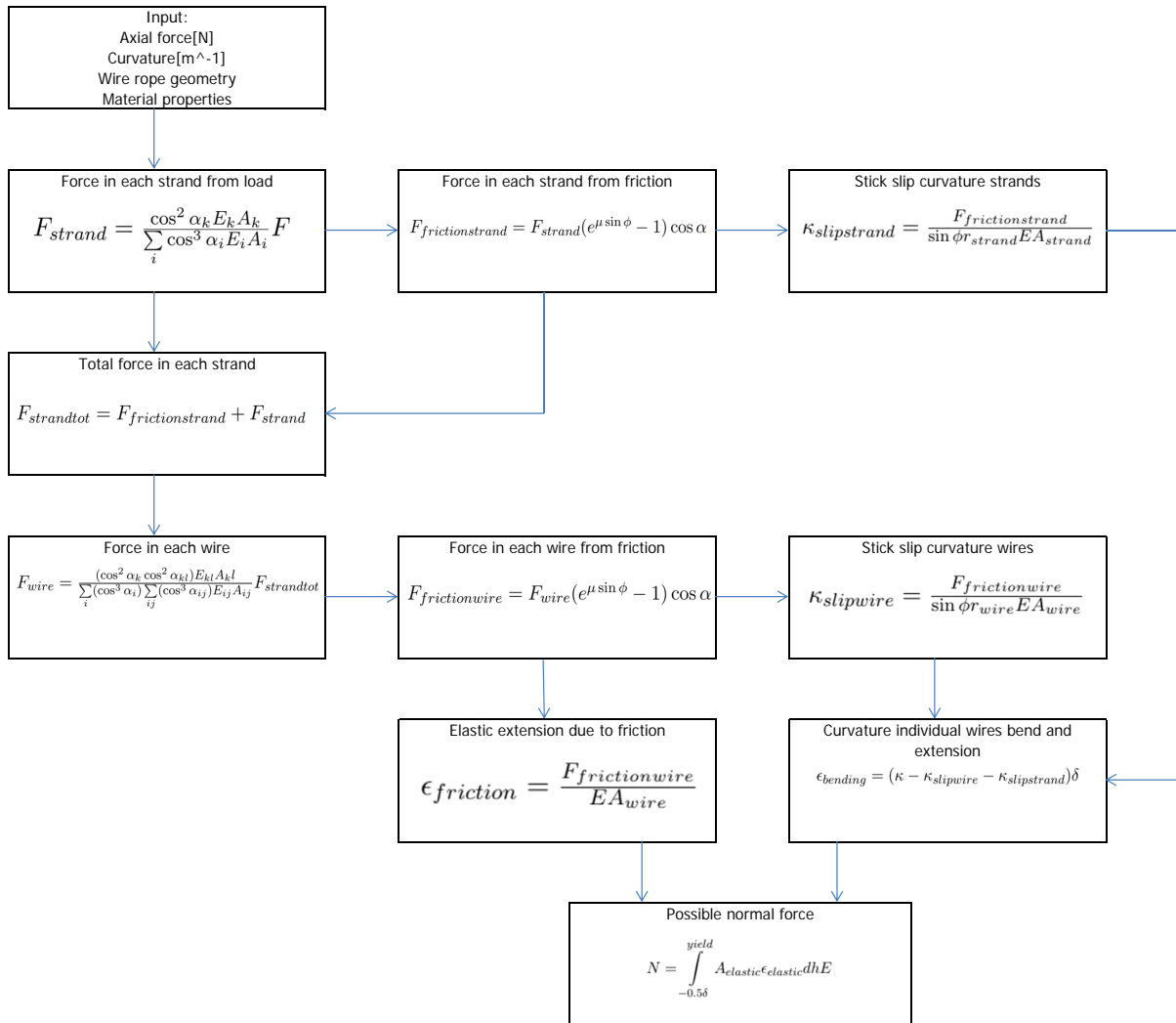


FIGURE 3.8: Flowchart Matlab

To get a good understanding of what effect the different parameters in the model have four wire ropes have been modelled and the results are shown in figure 3.9, the DNV formula has also been included in each graph. A 6x36WS rope and a 6x18WS rope with a diameter of 20mm and 40mm are shown. These ropes have been modelled with varying friction coefficients, wire tension and $\frac{D}{d}$ ratio's. The outcome is the reduction in capacity. It should be noted that the mentioned wire stress is only used to calculate friction effects. The actual tension force is not included in the capacity reduction. This stress is based on the stress that would occur in the central wire of the wire rope. The value for capacity reduction is based on the wire that has the highest capacity reduction as explained in paragraph 3.4. A realistic wire rope is best modelled by the graphs with $\sigma=500 \frac{N}{mm^2}$ (based on a safety factor of 4) and $\mu=0.15$.

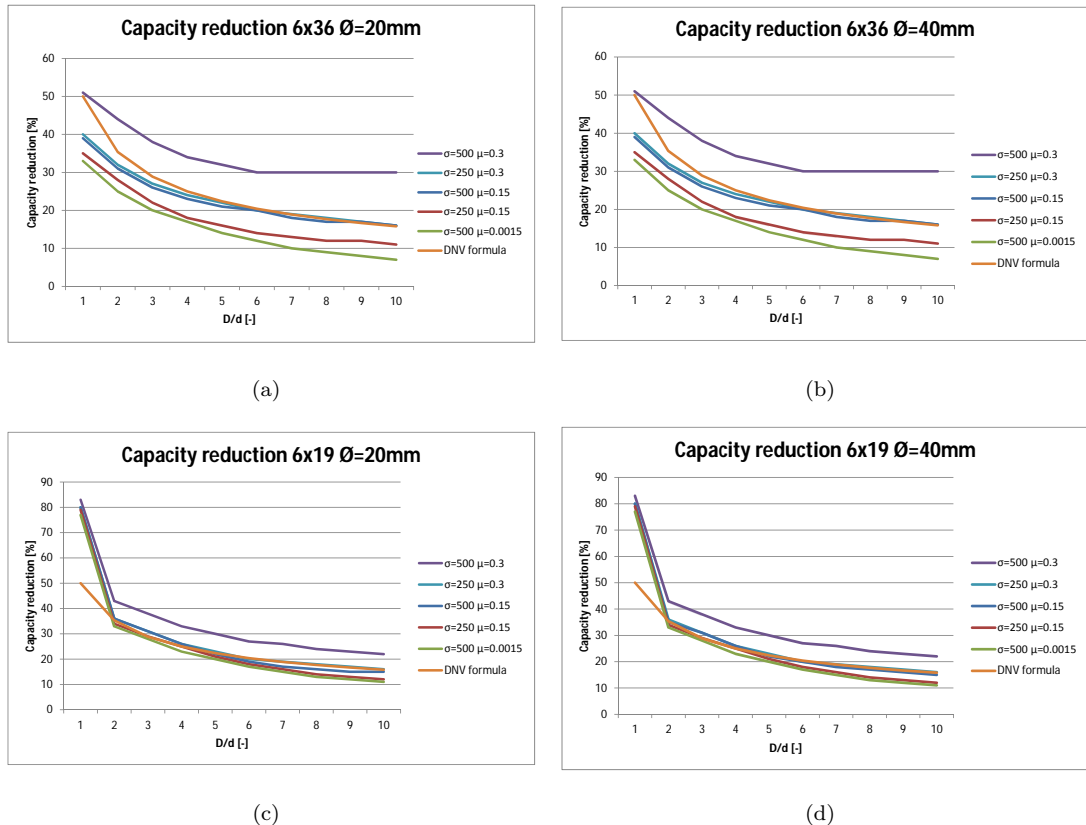


FIGURE 3.9: Capacity reduction versus $\frac{D}{d}$ ratio for analytical model versus DNV formula of (a) 6x36WS $d=20\text{mm}$ (b) 6x36WS $d=40\text{mm}$ (c) 6x19WS $d=20\text{mm}$ (d) 6x19WS $d=40\text{mm}$

To make a fair comparison between the analytical model and the DNV formula an adjustment has to be made. The norm set by DNV is based on the lowest 5th percentile values [14], while the analytical model is based on average values. To obtain similar 5th percentile values for the analytical model the input values have been modified to their characteristic 5% values. For the model in this thesis the ultimate tensile strength has

been lowered by 10%, this is based on the variation of tensile strength as described in [19]. This produces a graph as shown in figure 3.10.

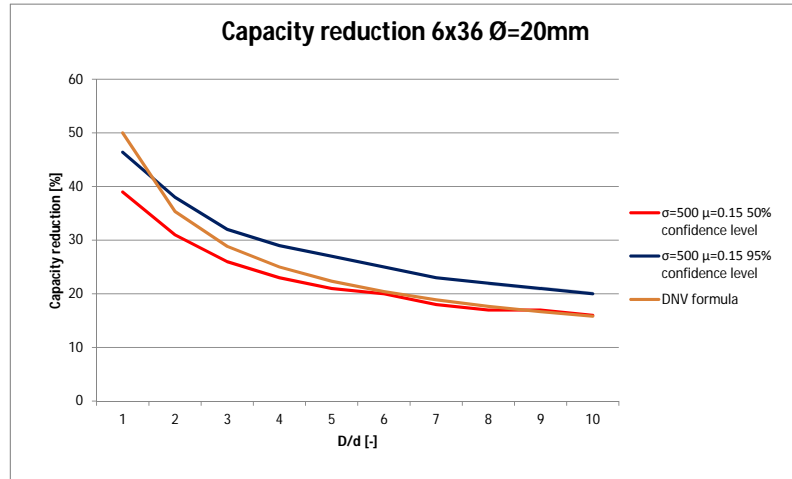


FIGURE 3.10: Capacity reduction versus $\frac{D}{d}$ ratio for analytical model with 50% and 95% confidence level

3.7 Conclusions from the analytical model

From fig 3.9 several conclusions on the bending behaviour of wire rope can be drawn. As expected a higher friction coefficient causes wires to stick longer and have larger strains. Applying a higher axial force seems to have the same effect as a higher friction coefficient. For this reason the graph of $\sigma=500 \frac{N}{mm^2}$ with $\mu=0.15$ overlaps with the graphs of $\sigma=250 \frac{N}{mm^2}$ with $\mu=0.30$.

Every graph seems to approach a constant value, this is most clear for the graphs with higher friction and axial force. This value is based on the strain developed during the sticking phase, because this value is reached at $\frac{D}{d}$ values of 30. It appears as a constant value in the graphs.

The 6x36 rope consists of more smaller diameter wires than the 6x19 rope. The effect of this becomes clear at $\frac{D}{d}$ values of one. The 6x19 rope has a sharp increase in reduction factor to approximately 80%. This is because the greater diameter wires almost reach their ultimate strain of 3% due to bending and friction effects. The amount of strain left before wire break only allows a very limited normal force in the wires. An important conclusion here is that not only the wire rope diameter matters, but also the wire diameter.

The influence of higher $\frac{D}{d}$ ratios is quite obvious and as expected. Higher values have a lower reduction. In the case of low friction this reduction approaches zero percent.

If both the rope diameter and the diameter of the bend are doubled, keeping a constant $\frac{D}{d}$ ratio, the reduction factor stays the same. This suggest larger diameter ropes behave exactly the same as smaller diameter ropes as long as the diameter of the bend is adjusted at a similar rate as the rope diameter.

The place where the highest capacity reduction takes place and where failure is first expected also changes with the various parameters. If a certain layer has a large wire diameter the wire rope will fail here first. As the friction coefficient or the wire stress increases the failure shifts towards the center of the wire rope and to the center of the strands due to the stick effect.

The effect of the lack of wire diameter in the DNV formula has some serious implications. Comparing this graph with the formula from DNV gives some interesting results. For the 6x36 rope with $\frac{D}{d}$ ratios of 1 to 2 a difference in capacity reduction is present, up to 5% lower capacity reduction. For the 6x19 rope the opposite is true, leading to an increase in capacity reduction of roughly 30%. The wire diameter should be included in any reduction formula for bending.

The DNV formula also does not include wire tension or a friction coefficient. However, under normal use these parameters could be considered as constants, so this seems acceptable. At higher $\frac{D}{d}$ values where the wire diameter is not decisive the DNV formula matches closely with the results from the Matlab model.

Chapter 4

Model discussion

While modelling the wire rope some interesting concepts were discovered. In this chapter various subjects will be discussed that are related to the bending of wire rope, but did not fit in chapter 3. First the effect the load order has on the capacity reduction is investigated, the bending stiffness of cables is considered, the lifetime of cables is looked into, the influence of the lay length on the bending length and finally a short paragraph is written on the stumbling points encountered while attempting to construct a numerical model.

4.1 Load order

During the constructing of the analytical model it turned out that the order in which the loads are applied makes a difference. This also leads to a difference between the bending of slings and bending over shackles. In this paragraph the effect of the order is investigated. Before the order of the loads is considered a closer look is taken at the loads.

4.1.1 The loads

Two external loads are present, the bending and the normal force. The bending of the wire rope is a strain based load meaning the rope is bent to fit a certain curvature. This curvature causes a bending moment in the wire rope. The normal force in the wires is based on the externally applied force. The magnitude of this force is dependent on how much elastic strain the wire rope has left as explained in paragraph 3.4.

Besides these two external loads a third internal load can possibly develop, based on the order the loads are applied. This force is described in chapter 2 as the stick slip model by Papailiou. It is based on the friction between the wires and is extensively discussed in chapter 3. Depending on the tension in the wire rope the wires will stick together and will undergo larger strains over a certain curvature until they start slipping.

4.1.2 The order

With two external loads present there are two extreme cases in which the loads can be applied, namely.

- First axial load and then bending.
- First bending and then axial load.

If the axial load is applied first the wires grip onto each other, causing the wires to stick when they are bent. In other words, applying an axial load increases the bending stiffness. This causes the subsequent bending to create larger strains and thus a lower failure load. This effect increases towards the inside of the rope and the strands. Meaning the higher stresses and strains from this increase in stiffness occur on the inside of the rope.

If the wire rope is bent into its final form first and the axial load is applied afterwards, the bending stiffness will still increase. However, since no curvature is applied after the bending stiffness is increased, no additional strains are introduced in the wires. Figure 4.1 shows the difference in capacity reduction this change in load order causes for various stress states. The stress is the one calculated for the central wire of the central strand. A realistic stress for this wire is around $500 \frac{N}{mm^2}$.

4.1.3 Bending over a shackle

The main research question of this thesis refers to the bending of a steel wire rope over a shackle. In this case the question would be which of the two load orders matches that of a wire rope bend over a shackle. Figure 4.2 illustrates a wire rope bent over a shackle with a load being applied. The rope is bent first, but the final curvature is not reached until the axial load is applied. The additional strains from friction already develop at extremely low curvatures, equivalent to $\frac{D}{d}$ ratio's of 30. When the axial load is increased the curvature increases until it matches the shackle's curvature. Although the increase in curvature is small, it does allow the sticking forces to develop. For this reason it is

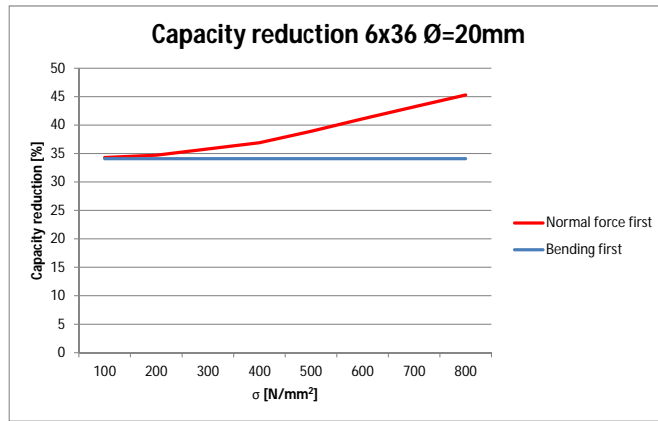


FIGURE 4.1: Reduction in capacity versus wire stress for the two different load orders,
 $\frac{D}{d}=1 \quad \mu=0.15 \quad d=20\text{mm}$

valid to consider the bending over a shackle as if the axial load is applied before the bending.

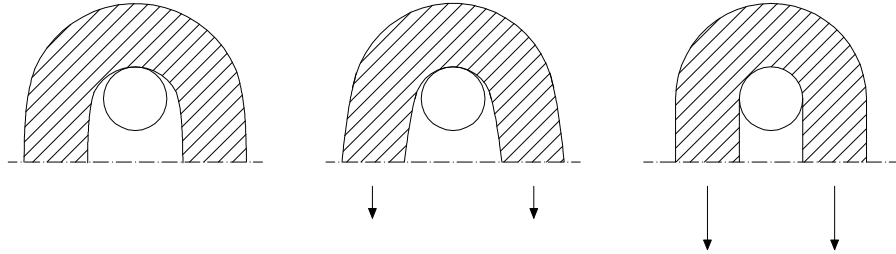


FIGURE 4.2: Wire curvature as axial load is applied

From figure 4.2 it can be seen that the curvature at the top of the wire rope remains constant during the loading and the curvature at the sides of the wire increases with loading as described above. This results in the maximum load occurring at the sides, where the wire rope runs onto the shackle. This would imply the wire rope would most likely fail here first. This is in compliance with experiments described in [15] where the wire rope would fail where the bend starts.

4.1.4 Slings

Slings are an often used end termination for cables. There are various ways for constructing a sling, figure 4.3 shows several types of often used slings. There are two points of interest in the sling that determine what reduction factor should be taken into account. The way the sling is connected to itself, this can either be by splicing the wire rope and weaving it back together, or simply by clamping the end of the wire rope to itself with a ferrule. In this thesis the exact effect of this loss is not investigated, but if

the reduction factor from this is the unfavourable one it should be used instead of the reduction factor for bending.

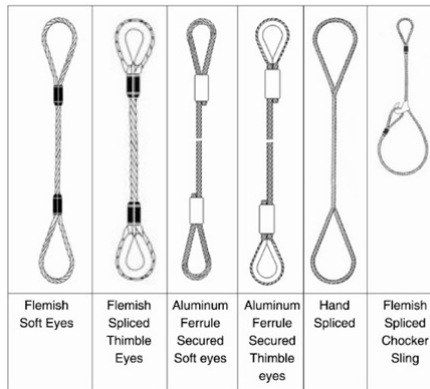


FIGURE 4.3: Different slings types

The second reduction factor is the one induced by the bending of the wire rope. It should be clear that for slings the bending of the wires occurs before any axial load is applied, see figure 4.4. Slings that are heavily loaded are secured with a thimble as shown in figure 4.4. This makes sure no further deformation takes place when the sling is loaded. This means no friction forces will occur, allowing the use of low reduction factor from figure 4.1.



FIGURE 4.4: Construction of a sling by splicing

4.1.5 Load order on material level

As discussed above the load order affects the overall wire rope mechanics. There is also an effect on the material level of the wire rope. This has to do with the fact that one load, the bending, is strain based and the axial load is force based. To understand the effect this has the material properties as displayed in figure 3.1 play an important role. For EIPS the first 1% strain generates forces. From the yield limit, 1% strain, to the maximum strain of 3% no additional forces are needed. If the strain based load is applied first, a high force is needed. If the strain based load is applied second, a much smaller force is needed, depending on how close to the yield limit the cross section is due to the force based load.

For both shackles and slings the strain based load is applied first. For slings there is no additional effect here, any leftover strain determines how much axial load can be applied. For the shackle the friction forces develop together with the axial load. The question is what part of the friction forces and the axial load develop before the yield limit is reached.

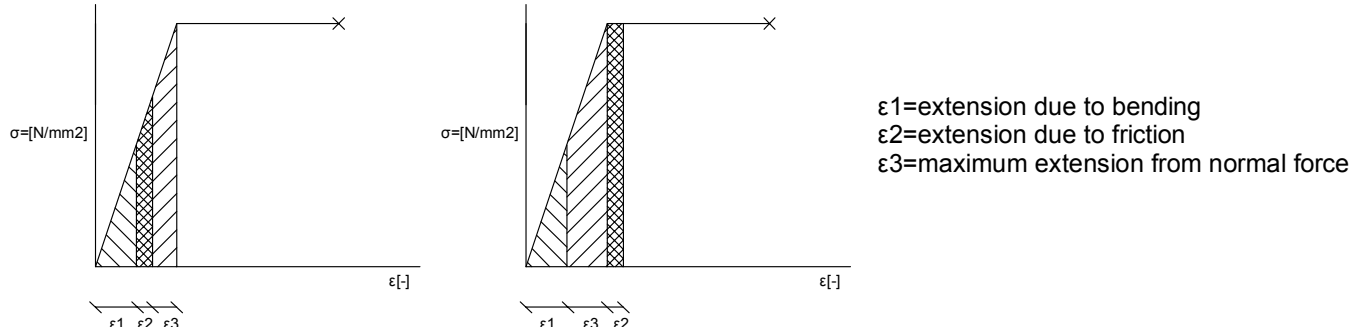


FIGURE 4.5: Effect of load order on material level

Figure 4.5 shows the two most extreme cases for the different load orders. In reality the friction force only develops with an increasing axial load. For this reason it is best to apply any strain from friction before considering the capacity left for a normal force. This explains why the strain from friction is applied before any axial load as shown in figure 3.2.

4.1.6 Conclusions from load order

Several interesting conclusions can be drawn from the impact the load order has. Applying an axial load before bending a wire rope increases the rope bending stiffness. This leads to higher strains and stresses in the wire rope, especially on the inside of the rope.

When bending the wire rope before applying any load there are no additional wire strains and stresses due to friction. It is important that the wire rope is secured against any additional deformation when the axial load is applied.

The bending of wire rope over shackles acts as if the axial load is applied before the bending. For slings the opposite is true. This leads to slings having a slightly lower reduction factor. Under a realistic loading this is about 5% to 7% lower, see figure 4.1.

When bend over a shackle it is expected the wire rope will fail at the sides of the shackle, where it enters the bend. This is because the curvature of the wire rope is able to increase during the loading, allowing the friction forces to develop.

On the material level there is a difference between applying a strain based load first or a force based load first. Applying the force based load first allows for a much higher force total force. This is because if the yield limit is reached any applied strain does not cause additional forces to develop.

4.2 Bending stiffness of wire rope

During the literature study many different attempts at modelling the bending stiffness of a wire rope were found. Most of these models are limited to describing only a single strand. In this chapter the theory developed by Papailiou [2] is used and extended to describe the bending stiffness of wire rope. Before delving into the mechanics a few important concepts that have to be considered when modelling the bending stiffness are mentioned.

- Initial rope settlement is highly non linear.
- Varying stiffness due to stick slip model.
- Bending stiffness dependent on axial load.
- Slip stick model causes bending stiffness to decline rapidly with increasing curvature.

4.2.1 Analytical model for bending stiffness

A newly constructed wire rope has a lot of empty space between the wires. Applying any load to the wire rope causes the cross section to contract until the wires are touching. Bending or extending a wire rope that has not settled yet will undergo very large deformations the first time it is loaded. For this model it is assumed any initial settlement is eliminated by pretensioning the wire rope.

There is a theoretical minimum and maximum to the bending stiffness a wire rope can potentially have. These are characterized by a bundle of loose wires versus a solid cross section. The formula to calculate these two is given in chapter 2, but repeated here.

$$EI_{regionI} = \sum_i \frac{n}{2} E A r^2 \cos^3 \alpha \quad (4.1)$$

$$EI_{regionII} = \sum_i n E \pi \frac{\delta^4}{64} \cos \alpha \quad (4.2)$$

n =number of wires [-]

A =surface of a wire [mm^2]

δ =diameter of wire [mm]

r =distance wire to center strand [mm]

α =lay angle wire [-]

Here $EI_{regionI}$ represents the stiffness of the loose wires and $EI_{regionII}$ of the solid cross section. As the curvature increases wires start slipping and the bending stiffness reduces. This slipping process is visualized in figure 4.6, the gaps developing between the wires and the strands indicate slipping.

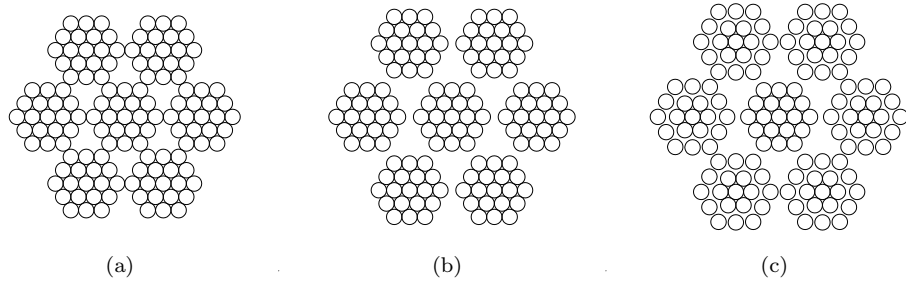


FIGURE 4.6: Slip order of the wires, gaps indicate slipping (a) no slip (b) strands slipping (c) outer layer of strands slipping

With the extremes known all the stiffness's lying in between have to be calculated. This is done using Steiner's theorem. The curvatures where a change in stiffness occurs are already known from the analytical model from chapter 3, these are known as the stick slip curvatures.

The assumptions for the analytical model of the bending stiffness are the same as for the capacity reduction with the following additions.

- Material is linear elastic. Bi linear material behaviour would complicate the model, while most of the time the bending stiffness is only required in the elastic zone.
- Initial settlement is not considered. Most wire ropes are preloaded to eliminate the initial settlement.

From this a bending stiffness that changes with the curvature is obtained. Figure 4.7 shows the bending stiffness for a 6x36WS and a 6x19WS wire rope. These wire ropes are modelled with $\sigma=500 \frac{\text{N}}{\text{mm}^2}$ and $\mu=0.15$.

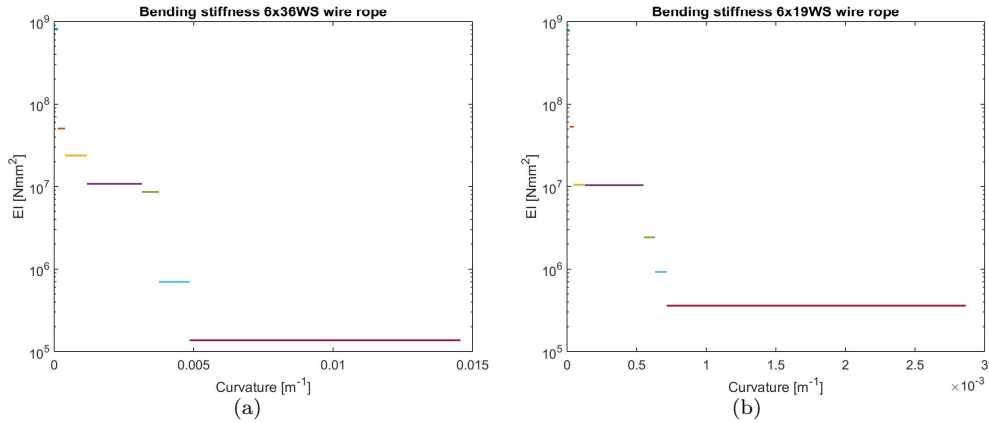


FIGURE 4.7: Bending stiffness [EI] versus curvature for $\sigma=500 \frac{N}{mm^2}$ and $\mu=0.15$ (a) 6x36WS wire rope $d=20$ mm (b) 6x19WS wire rope $d=20$ mm

4.2.2 Conclusion for bending stiffness

The bending stiffness of wire rope is a complicated problem that involves many different aspects of the rope. The above presents an idea of the factors that are involved and gives a method for calculating the bending stiffness. However with no experimental verification the validity of this model should be further investigated. Still some interesting conclusions can be drawn.

As should be clear by now the bending stiffness of a wire rope is not constant. It will vary between a maximum value, equal to the value of a solid cross section with the same surface, and a minimum value, equal to the bending stiffness of a bundle of loose wires.

The initial deformation of a wire rope is highly non linear due to wire settlement. Modelling this would be extremely complicated and rather futile since wire ropes are always preloaded to eliminate this initial settlement.

When wires start slipping the stiffness reduces. This slipping happens when the curvature of the wire rope increases. The exact curvatures where wire slip occurs depend on the friction coefficient μ between the wires and the axial tension applied to the wire rope.

The initial stiffness of the wire rope is very high, easily 1000 times higher than the minimum stiffness of the cable. The stiffness does decline rapidly however, after an initial curvature equal to a $\frac{D}{d}$ of 90 the minimum stiffness is already reached.

4.3 Influence of lay length

In paragraph 3.5 the influence of the helix structure is discussed. It is assumed the wires are in both the compression and the tension zone of the wire rope, causing the wires to not undergo any axial extension. In this paragraph the validity and the effect of this assumption are further investigated.

From figure 4.8(b) it can be seen that only half a lay length is needed for a wire to be completely in both the tension and compression zone. A rule of thumb is that the lay length of a wire rope is roughly equal to seven times its diameter. With this information the minimum $\frac{D}{d}$ ratio needed for a wire to be in both zones can be calculated.

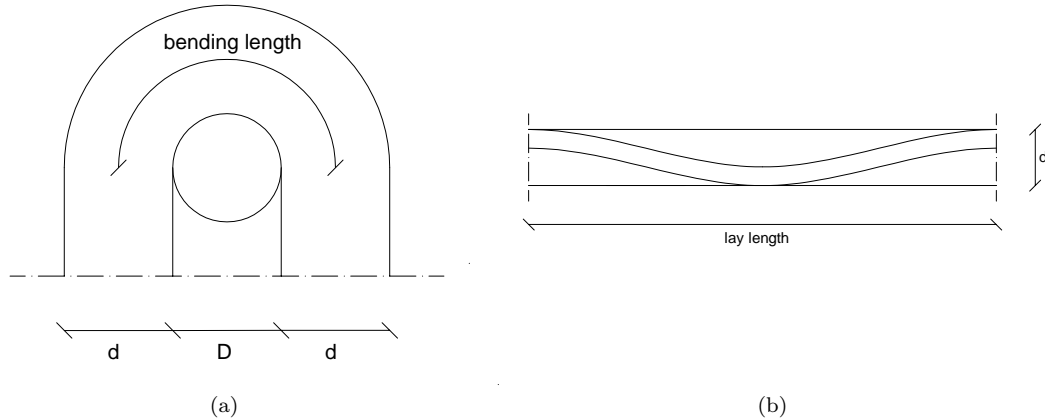


FIGURE 4.8: Wire rope (a) bending length (b) lay length

$$\text{laylength} > \text{bendinglength}$$

$$\begin{aligned} \frac{1}{2}\pi(d + D) &> \frac{1}{2}7d \\ \frac{D}{d} &> \frac{7}{\pi} - 1 = 1.23 \end{aligned} \quad (4.3)$$

From equation 4.3 it can be seen that a minimum $\frac{D}{d}$ ratio of 1.23 is needed for the helix to function properly. This value is based on a rule of thumb for the lay length of the wire so this value is not entirely accurate. In most cases $\frac{D}{d}$ will be a lot higher however, so it can be concluded that the assumption made in paragraph 3.5 is justified. When the $\frac{D}{d}$ ratio becomes smaller than 1.23 the helix structure starts to lose its function and the wire rope will act stiffer than described thus far. This increase in stiffness is seen when wire rope is bend around very small corners. When being bend over sharp corners

the wire rope will not adjust to the curvature of the corner. Instead due to the higher bending stiffness a larger curvature will be adopted by the wire rope.

4.4 Lifetime of wire rope

The lifetime of a wire rope is another concept that has not been touched upon yet in this thesis. In this paragraph the most important factors that influence the lifetime of a wire rope are discussed. Some of these effects are less important for the bending of wire rope as considered in this thesis, but will be mentioned here anyway. The effects are categorized as follows.

- Loss of lubrication.
- Strain ageing.
- Corrosion.
- Fatigue.
- Abrasion.

4.4.1 Loss of lubrication

Wire rope consists of many parts, a standard 6x36WS rope consists of over 250 wires that can all move relatively to one another. Lubrication is required to enable this movement. A wire rope is under tension most of its lifetime causing the wires to contract and squeeze out some lubrication. Below are the two most important functions of lubrication.

- Reduce friction as the individual wires move over each other.
- Provide corrosion protection in the core and inside wires and on the exterior surfaces.

Loss of lubrication will increase the friction coefficient leading to higher stresses when the wire rope is bent. Furthermore the wire rope will lose some of its protection against corrosion.

4.4.2 Strain ageing

Strain ageing can be triggered in heavily work-hardened carbon steel. General accepted is that strain ageing occurs due to the diffusion of carbon and/or nitrogen atoms to dislocations that have been generated by plastic deformation [20]. Over time this causes a further increase of the break strength of the steel, but a loss in ductility. This loss in ductility is important, because it might prevent the wire rope from redistributing the load between the wires. This process is visualized in figure 4.9.

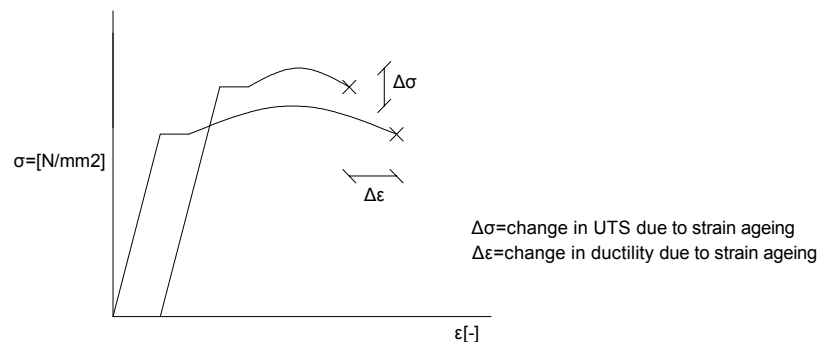


FIGURE 4.9: Stress strain diagram, increase of break strength at the cost of ductility due to strain ageing

4.4.3 Corrosion

Corrosion causes a decrease in cross sectional area of the wires, leading to a reduction in break load. Corrosion always occurs on the outside of a wire, so a wire rope consisting of many small wires will suffer more from corrosion because it has more exposed surface compared to a wire rope made of fewer large diameter wires. Since the wires are made from galvanized steel and are also protected by lubricant (if applied properly) corrosion damage is minimal when used in regular applications. When the ropes are used in seawater or a similar aggressive environment corrosion damage can cause considerable damage and limit the lifetime of a wire rope.

4.4.4 Fatigue

Fatigue is the growth of cracks in wires under repeated loading. It is an often discussed subject that can have a major influence on the lifetime of a wire rope. It is a dangerous failure mechanism since it is hard to predict when exactly failure will occur due to its statistical nature. For wire rope the fatigue limit is often reached by repeated bending

cycles, for example a wire rope running over a sheave, although repeated axial loading could also cause fatigue damage. Using many small wires lowers the stress range each wire goes through during a bending cycle leading to a higher fatigue load.

4.4.5 Abrasive wear

Abrasive wear can occur both on the inside and the outside of a wire rope. Internally it is caused by wires sliding over each other. On the outside it is caused by the wire rope sliding over sheaves, drums, or any other rough surface. The wear reduces the diameter of the wires and thus of the entire wire rope, leading to a reduction in breaking strength. Abrasion takes place on the surface of a wire. Reducing the surface, while keeping the total cross sectional area constant, limits the effect of abrasion. This can be done by applying fewer large diameter wires. Applying large diameter wires however has a negative effect on the resistance versus fatigue, this trade off is shown in figure 4.10.

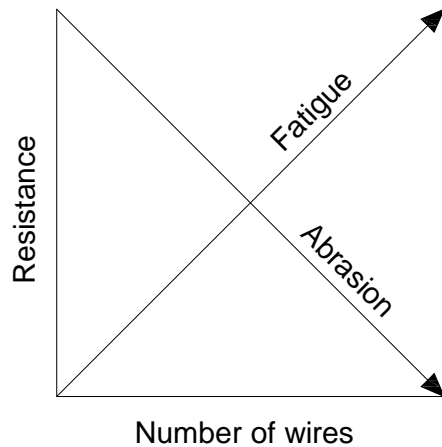


FIGURE 4.10: Effect of number of wires on abrasion and fatigue

4.5 Numerical modelling of wire rope

Complicated mechanical problems are often analysed with FE software. During the writing of this thesis attempts have been made to construct a FE model of the bending of wire rope. Eventually it was decided not to continue with the model. Although it is possible to construct a working FE model of wire rope, it is difficult, time consuming and needs to be validated to have some kind of practical use. Below are some stumbling points that should be considered when modelling wire rope.

The geometry of wire rope becomes complicated quickly. This has to do with the double helix structure. Simply inserting the correct geometry into a FE program can cause considerable trouble. A solution for this is to use a designated drawing program to draw the geometry and then import it into the FE program.

To produce an accurate model the interaction between the wires and the strands needs to be taken into account. For this each wire needs to be defined as a separate contact body and friction conditions needs to be defined between the different bodies. To accurately model friction a fine mesh is needed.

To model the effect of the helix structure correctly multiple lay lengths should be modelled. This requires a large length of wire rope to be modelled. In combination with the fine mesh required to model friction the computing time quickly grows out of hand. For this reason often a small length of the wire rope is modelled [17] [21] or only a single strand [16].

The boundary conditions are another problem. It is not feasible to model an entire wire rope with end terminations because this model would be too big. This means the boundary conditions need to represent the rest of the rope that would be attached to the model. To allow the wires to slide and move relatively to one another the boundaries should be modelled with springs. Obtaining the correct stiffness for these springs is complicated.

An alternative way to model the wire rope that should reduce computation time is to make use of semi-continuous models. This models the wire rope as multiple homogeneous hollow cylinders. This reduces the amount of elements needed significantly and makes the geometry a lot easier to model. Modelling the wire rope in such a way was not further investigated in this thesis.

Chapter 5

Experiments

To verify the analytical model developed in chapter 3, experiments are carried out. This chapter gives a description of the set-up of the experiments, the goal, observations during the experiments and their results. A statistical analysis is performed on the results. These results are used in chapter 6 to make a comparison with the theory and the DNV norm.

5.1 Goal of experiments

The goal of the experiments is to verify the analytical model developed in chapter 3. To accomplish this two experiments are carried out. First a small experiment is performed to confirm the test set-up will produce usable results and to obtain the break load of a straight wire rope. After this initial experiment an experiment is carried out to test the break load of a bent wire rope. These tests are performed on a 100 tons Losenhausen tensile testing machine at the laboratory of the Civil Engineering faculty in Delft. Figure 5.1 shows the tensile testing machine used.



FIGURE 5.1: 100 tons Losenhausen tensile testing machine

5.2 Experiment I

The goal of experiment I is to verify the test set-up. A table of the test specimen is shown in figure 5.2(a). This test is performed first for various reasons. The exact failure load of a straight wire rope is needed to compare this with a bent wire rope. The second reason is the length between the clamps of the tensile testing machine is limited and it is unknown how this will influence failure of the wire rope. In case every specimen fails at the sockets the test results are useless. Therefore this test is performed before the second experiment. Figure 5.2(b) gives an overview of the test set-up.

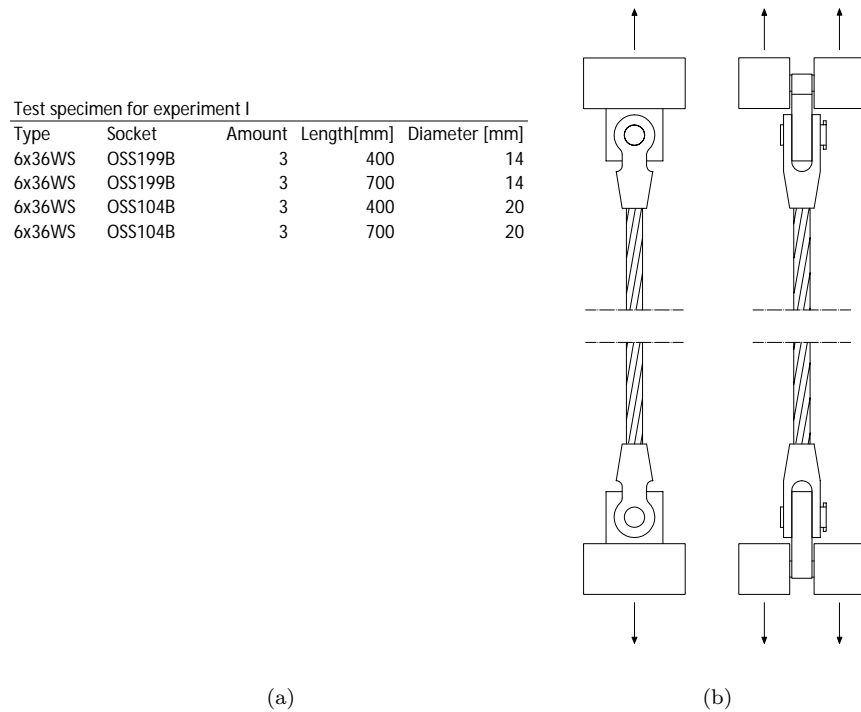


FIGURE 5.2: Overview experiment I (a) test specimen (b) overview test set-up

5.3 Results and observations experiment I

The first experiment was performed on 8 July 2015 in the Stevin II laboratory of the civil engineering faculty of TU Delft. The test results are displayed in table 5.1. Figure 5.3 shows pictures that were taken during the experiment.

Overall the execution of the experiments went very smoothly, there were some minor problems with fitting everything in the tensile testing machine. For the first 14mm test sample the force measuring scale was set-up incorrectly, producing a break load roughly half the MBL. This load was scaled back afterwards, but it might be slightly inaccurate. This could explain the higher standard deviation for the d=14 mm cables.

(a)		(b)	
Sample number	Straight Ø14 wire rope break load [kN]	Sample number	Straight Ø20 wire rope break load [kN]
1	173	7	314
2	167	8	330
3	170	9	319
4	166	10	322
5	165	11	324
6	159	12	322

TABLE 5.1: Overview experiment I results (a) d=14 mm (b) d=20 mm

FIGURE 5.3: Photographs test specimen (a) (b) (c) specimen number 4, d=14 mm (d)
(e) (f) specimen number 7, d=20 mm

Every single break load measured is higher than or equal to the MBL given by the manufacturer. More importantly, not a single specimen failed at the socket.

There appeared to be no real difference between the break load of the 500 mm samples and the 700 mm samples. For this reason the different lengths are combined in table 5.1(a) and (b).

During the experiment the snapping of wires could be heard at 90% of the break load of the wire rope. No wires could be seen breaking, indicating that it was the core of the wire rope that was failing first.

A statistical analysis shows that for the ropes with $d=14$ mm there are deviations up to 5% in the break load. As mentioned earlier this might be caused by an incorrect scale for the first sample, which has a very high variance. The ropes with $d=20$ mm show less variation, only up to 3%.

With the actual break load of the wire ropes known and the fact that the samples do not fail at the sockets the second experiment can be set up.

5.4 Experiment II

The goal of the second experiment is to obtain the reduction factor for a wire rope bent over a shackle. A table of the test specimen is shown in figure 5.4(a). The goal of this test is to obtain the break load of a wire rope that is bent with different $\frac{D}{d}$ ratios. For this experiment three different $\frac{D}{d}$ ratios are tested, namely 1, 1.5 and 2. The reason these are chosen is because low $\frac{D}{d}$ ratios are the ones that are most often used.

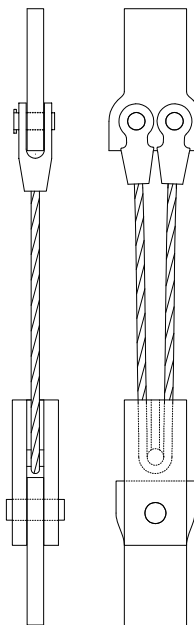
The obtained break load can then be compared with the break load of a straight wire rope as obtained in experiment I. To perform this test some auxiliary pieces had to be constructed. The test set-up can be seen in figure 5.4. In appendix C all the pieces used for this test are shown. The test set-up is designed to simulate a wire rope bent over a shackle. However no actual shackle is used because this would be difficult to fit into the tensile testing machine and it would not be possible to reach all the desired $\frac{D}{d}$ ratios.

5.5 Results and observations experiment II

After some delay the second experiment was performed on 8 October 2015 in the Stevin II laboratory of the civil engineering faculty of TU Delft. The test results are displayed in table 5.2. Figure 5.5 shows pictures that were taken during the experiment.

No problems were encountered during the execution of the experiment.

Test specimen for experiment II					
Type	Socket	Amount	Length [mm]	Diameter [mm]	D/d [-]
6x36WS	OSS199B	3	1200	14	1
6x36WS	OSS199B	3	1200	14	1.5
6x36WS	OSS199B	3	1200	14	2
6x36WS	OSS104B	3	1200	20	1
6x36WS	OSS104B	3	1200	20	1.5
6x36WS	OSS104B	3	1200	20	2



(a)

(b)

FIGURE 5.4: Overview experiment II (a) test specimen (b) overview test set-up

(a)			(b)		
Bent Ø14 wire rope break load			Bent Ø20 wire rope break load		
D/d ratio	Sample number	Break load [kN]	D/d ratio	Sample number	Break load [kN]
1	1	210	1.5	1	420
	2	208		2	400
	3	215		3	411
1.5	4	223	2	4	410
	5	220		5	405
	6	210		6	415
2	7	215	2	7	430
	8	220		8	425
	9	225		9	430

TABLE 5.2: Overview experiment II results (a) d=14 mm (b) d=20 mm

At roughly 25% of the break load the wire rope had changed its shape from figure 5.5 (a) to (b).

As with the straight wire ropes, the breaking of individual wires could be heard at 90% to 95% of the break load. No wires were observed breaking, indicating that it was the core breaking first. However visibility on the bent part of the cable was limited due to the test set-up and safety concerns.

Wire rope ovalization was observed during the test. Looking at the test specimen after failure flattening of the individual wires was limited. This indicates the ovalization occurred mainly through the wires being displaced.

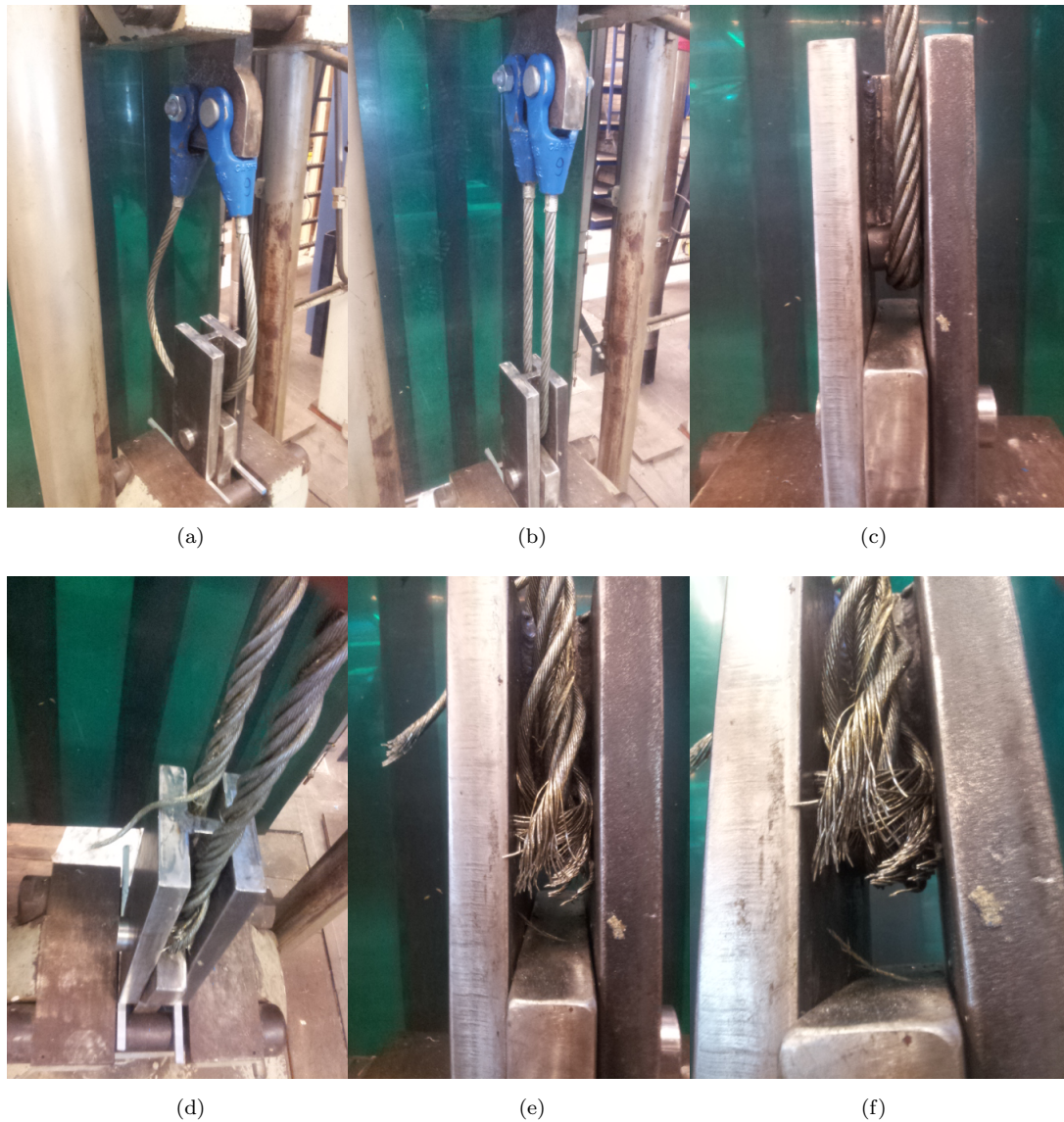


FIGURE 5.5: Photographs test specimen 9, $d=20$ mm $\frac{D}{d}=2$ (a) before test (b)(c) during test (d)(e)(f) after test

All wire ropes failed at the bend. When breaking a loud bang was heard together with sparks appearing at the point of breaking. Small wire parts were flying up to 3 meters from the testing machine. All wires had 1 to 3 strands remaining after breaking, the core of the wire ropes was broken in all the specimen.

5.6 Statistical analysis

To make any comparison between the experimental data, the analytical model and the DNV formula a confidence interval and a P-value are calculated for the test data. This is

done by making use of Student's t-test [22], see 5.1. This test is based on the assumption that the test results follow a normal distribution.

$$\bar{x} = \frac{\sum x}{n}$$

$$\sigma = \sqrt{\frac{\sum(x - \bar{x})^2}{n}}$$

$$P(95\%) = \bar{x} - t_{95\%} \frac{\sigma}{\sqrt{n}}, \bar{x} + t_{95\%} \frac{\sigma}{\sqrt{n}} \quad (5.1)$$

$P(95\%)=95\% \text{ confidence interval } [-]$

$x=\text{test results } [\text{kN}]$

$\bar{x}=\text{average of test results } [\text{kN}]$

$\sigma=\text{standard deviation } [\text{kN}]$

$n=\text{number of test specimen } [\text{kN}]$

$t_{95\%}=4.3 \text{ parameter that defines } 95\% \text{ confidence interval } [-]$

The reduction factor can now be calculated according to 5.2. The confidence interval of the capacity reduction for 14mm and 20mm wire ropes is shown in figure 5.2.

$$R = 1 - \frac{F_{bent}}{F_{straight}} \quad (5.2)$$

$R=\text{capacity reduction of a bent cable } [-]$

$F_{bent}=\text{break load of a bent cable } [\text{kN}]$

$F_{straight}=\text{break load of straight cable } [\text{kN}]$

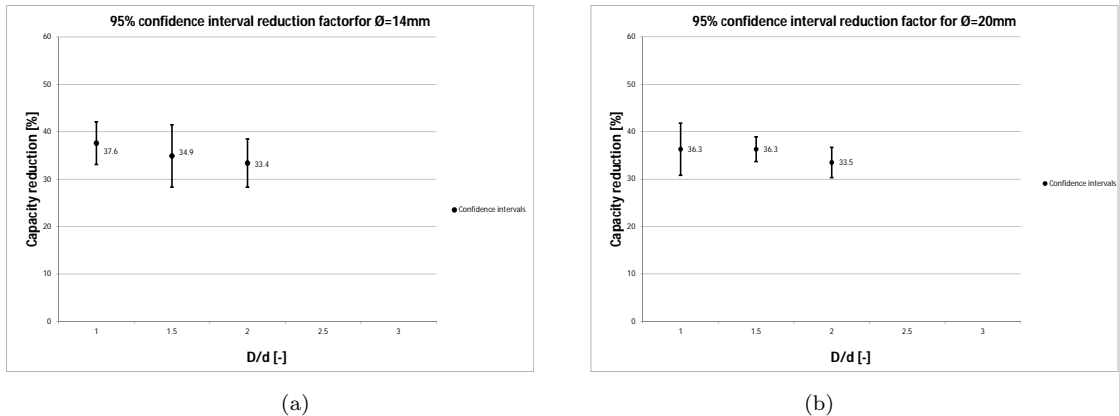


FIGURE 5.6: Confidence interval for reduction factor (a) $d=14\text{mm}$ (b) $d=20\text{mm}$

In addition to the confidence interval a P-value is calculated. The P-value allows us to quantify the worth of the tested hypothesis versus the experimental data. In this case the analytical model with a confidence level of 50% is tested versus the averages of the experiments. The P-values of these hypothesis are shown in table 5.3.

For the analytical model:

$$H_0 : R_{analytical} = \mu_{experiments}$$

$$H_1 : R_{analytical} \neq \mu_{experiments}$$

P value for analytical model with a 50% confidence level		
Ø14		
D/d	P-value	Defintion
1	0.0763	Statistically not quite different
1.5	0.9559	Statistically not different
2	0.0901	Statistically not quite different
Ø20		
D/d	P-value	Defintion
1	0.1230	Statistically not different
1.5	0.1340	Statistically not different
2	0.0055	Statistically very different

TABLE 5.3: P-values for analytical model with 50% confidence level

Chapter 6

Comparison between theory and experiments

In chapter 3 an analytical model was constructed, the results of this model and a comparison with the DNV formula are also discussed in chapter 3. In chapter 5 the experiments that were executed are discussed and a confidence interval as well as a P-value is calculated. In this chapter a comparison is made between the experiments, the theoretical model and the DNV formula. Before this a short paragraph is written about general observations.

6.1 Comparison general wire rope theory with experiments

While testing the straight wire ropes a break load was found slightly higher than the MBL given by the manufacturer. This seems reasonable since the manufacturer might include some extra safety to be sure no accidents happen.

All wire ropes did not fail at the socket. The resin connection between the wire rope and the socket is stronger than the wire rope itself.

At roughly 90% of the break load the sound of wires breaking could be heard. No wires could be seen breaking, indicating the wires on the inside of the wire rope were breaking. This matches general wire rope theory, where the wires in a single helix or a smaller helix angle are the first ones to break.

Once the core has failed the rest of the wire rope fails almost instantly. There is no redistribution possible between the wires in the outer strands. This matches with the material properties showing little plastic deformation capacity.

6.2 Comparison of the analytical model with experiments

In figure 6.1 the confidence intervals as calculated in chapter 5 are plotted together with the most realistic graph from the model as discussed in chapter 3 for a 50% and a 95% confidence level ($\sigma=500 \frac{N}{mm^2}$ and $\mu=0.15$).

From figure 6.1 (a) and (b) it can be seen that there is a good match between the analytical model with a 50% confidence level and the averages of the experiments. The analytical model with a 95% confidence level shows a decent match with the maximum value of the confidence interval. From this it can be concluded that the bending of wire rope as described in this thesis is a promising way to model wire rope.

This leads to a few other interesting conclusions. The effect of friction in wire rope is an often discussed topic. In the theoretical model the influence of friction is taken into account which leads to an increase of roughly 5% to 10% in capacity reduction. This increase in capacity reduction is directly related to the bending stiffness of a wire rope as discussed in chapter 4. No experiments to test the bending stiffness are performed, but it gives a good indication that the way bending stiffness is modelled is close to the actual value.

According to the theoretical model there is no difference in the diameter of the cable. From the experiments no difference can be observed between the 14mm and 20mm wire ropes. Since the difference in diameter is quite small it can not be confirmed that this effect translates to larger diameter wire ropes.

In the model it is assumed rope ovalization has a minimal effect and is not taken into account. Although ovalization of the entire wire rope is observed during the experiments, flattening of the individual wires is limited. This means the total area of the cross section and bending stiffness of the wires rope do not change much and the assumption is justified.

6.3 Comparison with DNV formula

In figure 6.2 the DNV formula is added to the confidence interval and the analytical model.

When looking at the DNV formula and the analytical model with a 95% confidence level it can be seen that they do not deviate much to begin with. At a $\frac{D}{d}$ ratio of 1 the theoretical model predicts a 5% lower capacity reduction, this shows a better match with the experimental value. At a $\frac{D}{d}$ of 1.5 the analytical model and the DNV formula

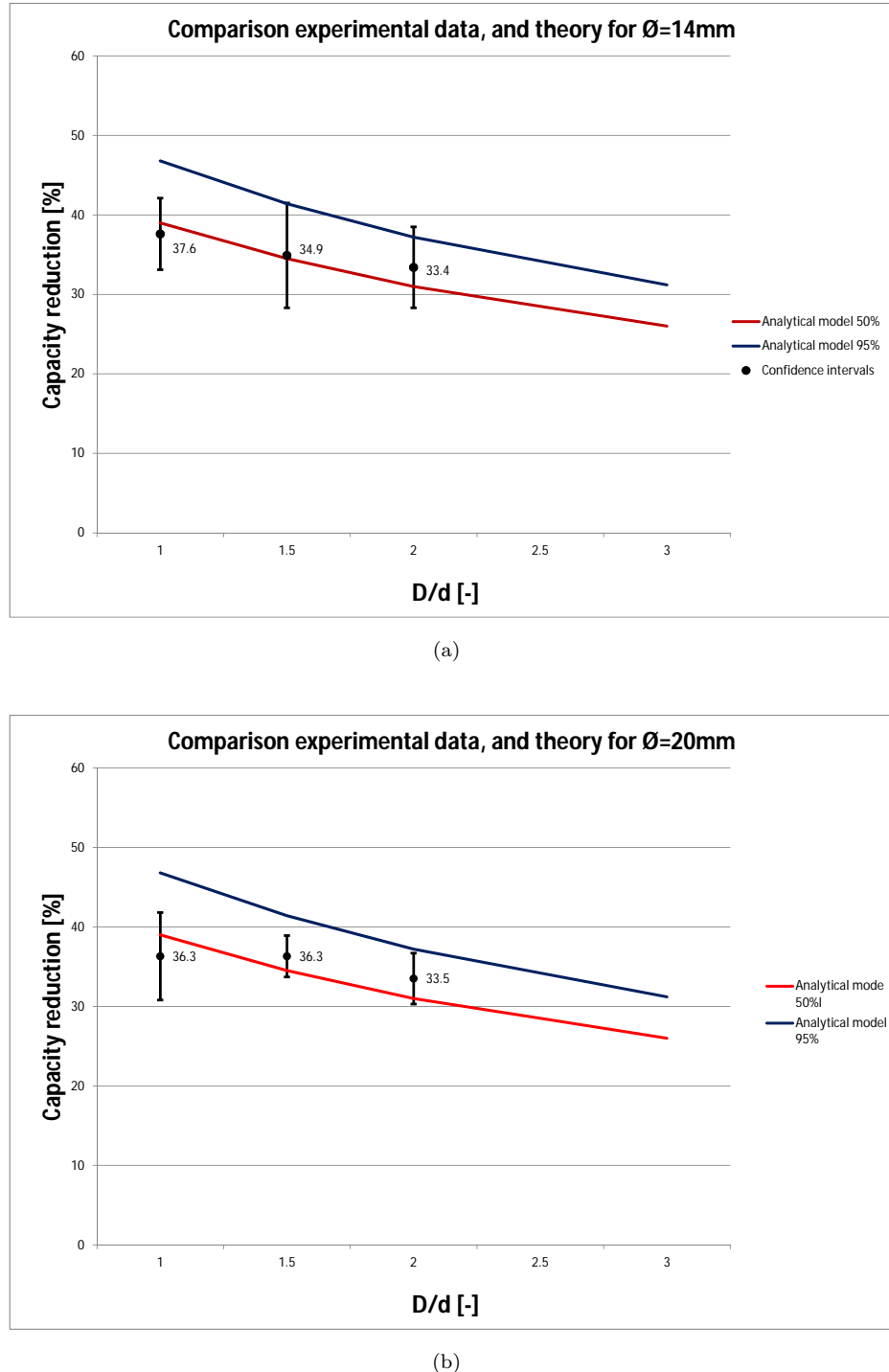


FIGURE 6.1: Reduction factor versus $\frac{D}{d}$ ratio for confidence interval of experiments and analytical model with 50% and 95% confidence level (a) $d=14\text{mm}$ (b) $d=20\text{mm}$

show a good match with the experimental value being slightly lower. at a $\frac{D}{d}$ value of 2 the analytical model shows a higher capacity reduction than the DNV formula. With the difference being so small it is not possible to confirm this. The confidence interval of the experiments does exceed the DNV formula slightly at $\frac{D}{d}$ values of 2, this could

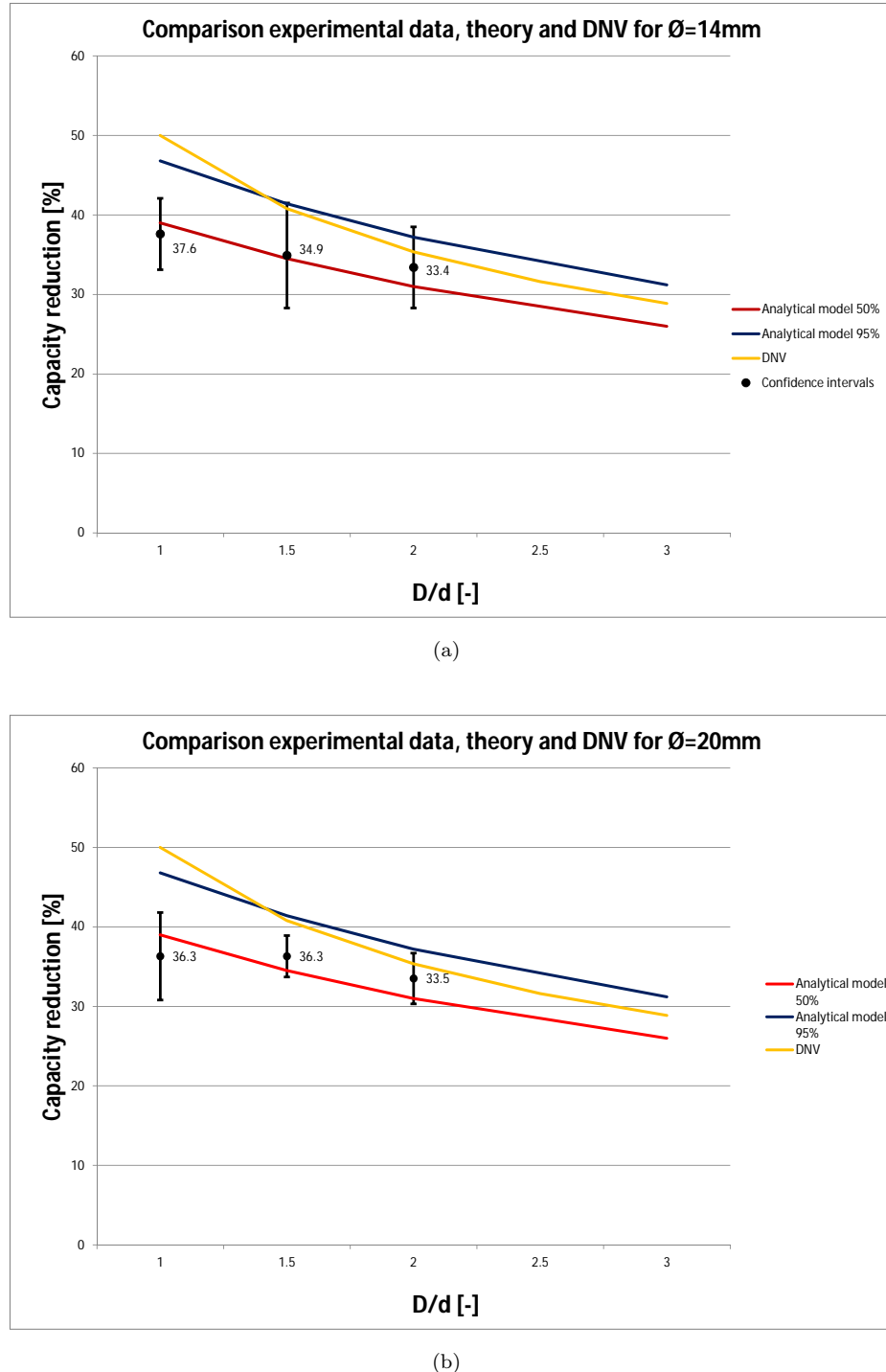


FIGURE 6.2: Reduction factor versus $\frac{D}{d}$ ratio for confidence interval of experiments, analytical model with 50% and 95% confidence level and DNV formula
 (a) $d=14\text{mm}$
 (b) $d=20\text{mm}$

indicate that the DNV formula is unsafe in this region. However the sample size of the experiments was small, this leads to high standard deviations, which could also be the cause of this.

Chapter 7

Conclusion, discussion and recommendation

In this final chapter the conclusion, discussion and recommendation of this thesis are presented. First the main and secondary research question are answered and additional conclusions are drawn. Then discussion points are mentioned. Finally a recommendation for further research is given.

7.1 Conclusion

With the knowledge obtained from constructing the analytical model the main and secondary research question can be answered.

How does the forced bending of a steel wire rope around a shackle affect the break load of the wire rope?

The break load of a bent wire rope is affected by much more than one might first suspect, namely the axial tension, friction coefficient, wire diameters, total wire rope diameter and the $\frac{D}{d}$ ratio.

The reduction in capacity is dominated by the effect of individual wires being bent, similar to a bundle of loose beams being bent. Plastic deformation needs to be taken into account to build a model that accurately describes smaller $\frac{D}{d}$ ratios.

Due to the helix structure axial tension causes friction forces to develop between the strands and the wires. This increases the stiffness of the wire rope and leads to higher stresses and strains when the wire rope is bent. As soon as the wires start slipping the

stiffness lowers drastically and any further deformation causes much lower stresses and strains.

The build up of the wire rope plays a role in the capacity reduction, especially the size of the wires. If the wires become too large and the rope is bent over a small diameter the plastic deformation capacity is reached and this leads to a sharp decrease in the capacity of the rope.

How does the forced bending of a steel wire rope relate to the reduction factor for bending enforced by DNV?

The analytical model developed matches the norm set by DNV quite well, showing only small differences. At $\frac{D}{d}$ ratios 1 analytical predicts a slightly lower capacity reduction, roughly 5%. At $\frac{D}{d}$ ratios of 2 and higher the analytical model predicts a higher capacity reduction.

The big difference between the model and the DNV formula is the parameters that are considered. In the DNV formula only the diameter of the wire rope and of the bend are considered. Not including axial tension and friction coefficient is acceptable since these could be considered as constant values for steel wire rope. Leaving out the wire diameter in the reduction formula for DNV is the biggest difference with the analytical model. Most wire rope configurations use sufficiently small wires, however with bigger wires and a small $\frac{D}{d}$ ratio a much higher reduction factor is obtained. This could lead to dangerous situations.

Experiments are performed for wire rope diameters of 14mm and 20mm at a $\frac{D}{d}$ of 1, 1.5 and 2. The results show a good match with the analytical model making it plausible that the theory as described in this thesis is a good way to model wire rope. When comparing the DNV formula with the experiments the lower capacity reduction at a $\frac{D}{d}$ of 1 can been seen in the experiments too. The slightly higher reduction factor for $\frac{D}{d}$ of 2 does show in the experiments, but with the small sample size of the conducted experiments it is hard to confirm this.

From the theoretical model it follows that the reduction factor does not change with wire rope diameters. While the experiments do not reject this statement, it could also not be confirmed due to the small difference in wire rope diameters being tested.

While not part of the main research, the bending stiffness was modelled by slightly extending the capacity reduction model. The result was a bending stiffness that rapidly declines as the wires start slipping. While not experimentally validated the fact that the capacity reduction model seems accurate indicates that this model is a promising way to model the bending stiffness of wire rope.

The difference between a shackle and a sling is that a sling is already preformed to the desired bending radius. While bending over a shackle the wire rope still needs to adjust this radius. This movement allows the friction forces to develop. This means that slings have a slightly lower capacity reduction than a wire rope bent over a shackle.

7.2 Discussion

To construct an analytical model that predicts the loss in capacity due to bending certain assumptions have to be made. One of these assumptions is a linear friction model. The real behaviour of friction is far more difficult than a simple linear model. Another assumption on friction is that wires in the same layer do not touch. While there is a theoretical foundation for this, it seems hard to believe that when looking at an actual wire rope no such contact occurs.

Another assumption is that rope ovalization can be ignored, because it is assumed the diameter of the wire rope matches that of the shackle. This does not seem to be the case in most applications. In the experiments a pin was used and not a shackle allowing the cross section of the rope to deform. Rope ovalization was observed during the experiment, although flattening of the wires was very limited.

The curvature used to calculate wire bending for each wire is assumed to be the curvature adopted by the central wire of the wire rope. For small $\frac{D}{d}$ ratios the inner wire experiences a larger curvature than the outer wire and this assumption becomes inaccurate.

Plastic deformation of individual wires is taken into account in the model. However redistribution of forces between wires due to plastic deformation is not taken into account. The way failure occurred almost instantly during the experiments indicates that not much redistribution is possible, although some further research into the possible redistribution of loads could give more insight in the failure mechanism.

The test specimen used for the experiments are all ordered at the same manufacturer. It is likely that the individual pieces of wire rope are cut from the same original wire rope. This leads to all the wire ropes having similar production errors and this makes the test less representable for all wire ropes. A more accurate test would include wire ropes from different rolls of wire rope and from different manufacturers.

7.3 Recommendation

According to the theoretical model developed in this thesis large diameter wire ropes would behave exactly the same as smaller diameter ropes. During the initial phase of this master thesis there were plans to extend the experiments to large diameter wire ropes. A much larger tensile testing machine is needed for this. For diameters up to 90 mm a 1000 tons tensile machine is needed. This plan was later abandoned due to time and budget constraints. Still it would be interesting to see how small diameter wire ropes relate to large diameter wires ropes.

The bending stiffness is an important characteristic of wire rope that defines the behaviour of the cable in different applications where wire rope is bent or twisted. The topic of bending stiffness is addressed in papers in various ways, however there is no final answer to what the bending stiffness of a wire rope is. In this thesis an attempt is made to quantify the bending stiffness based on the model used for capacity loss due to bending. The model presented in this thesis looks promising and could be further developed to predict the bending stiffness more accurately. Performing experiments to obtain the bending stiffness of cables would be required to verify such a model.

Further research on the effect of friction in wire ropes could provide a much better insight on what happens inside a wire rope. The magnitude of the friction between the wires defines the transition between stick and slip state which has a large impact on the bending stiffness and the capacity reduction when the wire rope is bent. Making use of static and dynamic friction coefficients as well as a more accurate friction coefficient could improve the model.

A FE model could give a much better idea on the functioning of wire rope. Since it is not possible to look or measure the inside of a wire rope during experiments. Numerical models might be able to explain this. The stress/strain distribution between the wires in the cross section and magnitude of the friction would be interesting to know.

Appendix A

Material properties EIPS

The cable manufacturer Bridon performed a tension test on a 2.8 mm diameter steel rod with a steel quality of 1960 $\frac{N}{mm^2}$. The exact conditions of the test are not known. The data matches the expectations and it is acceptable to assume a renown cable manufacturer provides reliable test data. Any other sources of information on the material properties of EIPS were not considered reliable. For this reason the material properties are completely based on this test. The stress strain diagram from the tension test is shown in figure A.1.

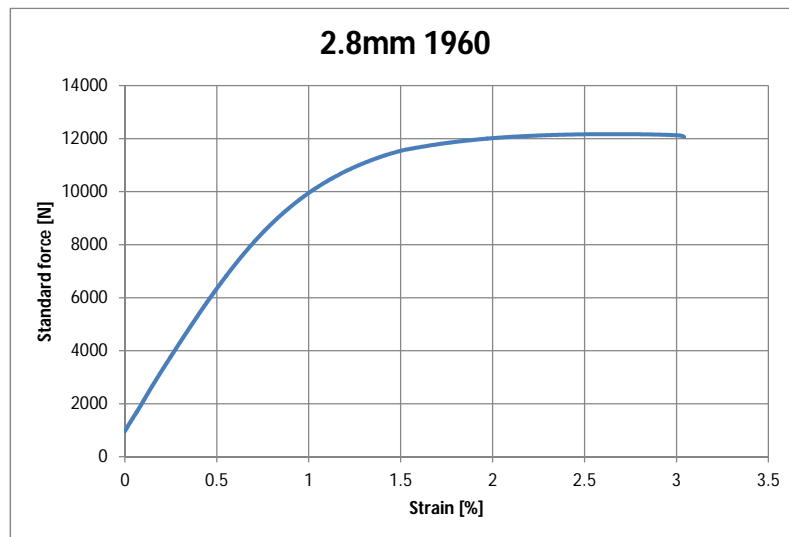


FIGURE A.1: Stress strain diagram from tensile test performed by Bridon for steel quality 1960 $\frac{N}{mm^2}$ loaded until break

From this stress strain diagram it was chosen to model the steel with a bi-linear stress strain diagram as shown in figure A.2. The bi-linear model is chosen because it matches the actual stress strain diagram quite well and is easy to incorporate in the Matlab model. A more complicated diagram would only be slightly more accurate, but a lot more complicated to model.

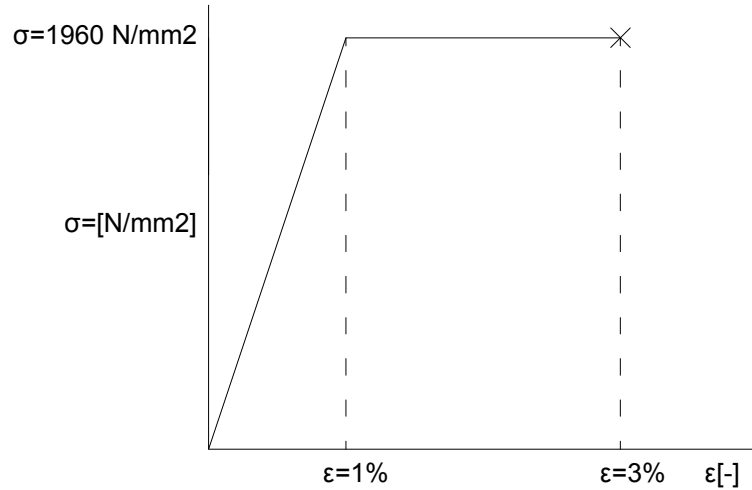


FIGURE A.2: Stress-strain diagram of EIPS used for modelling

Appendix B

Set up experiment I

In this appendix an overview is given of the equipment used to perform experiment I. Two sets of auxiliary steel plates are required to attach the cables to the tension machine. The design of these plates is also given in this appendix. Figure B.1 shows the two sets of plates used, these plates have a safe working load of 180 kN and 370 kN respectively. Figure B.2 shows the test set up used to perform experiment I.

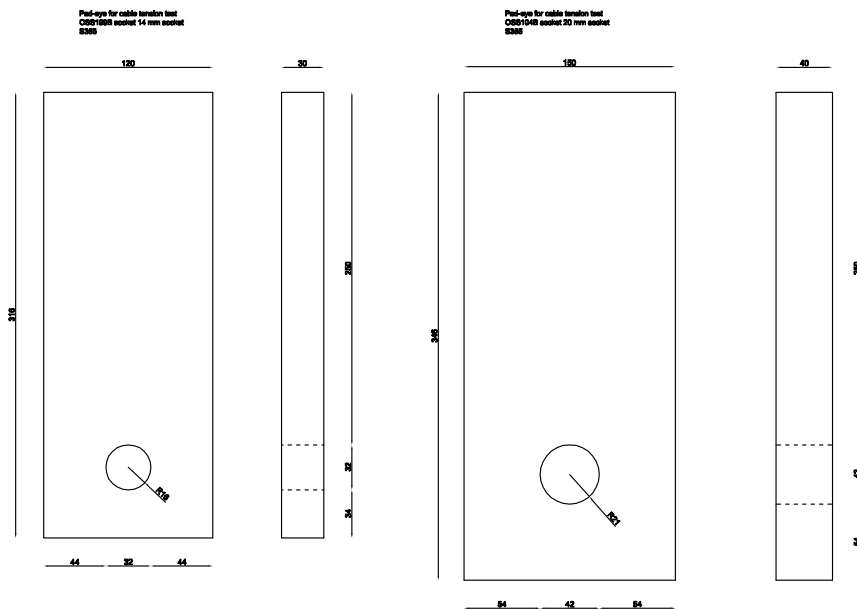


FIGURE B.1: Plates for attaching cables to tensile machine

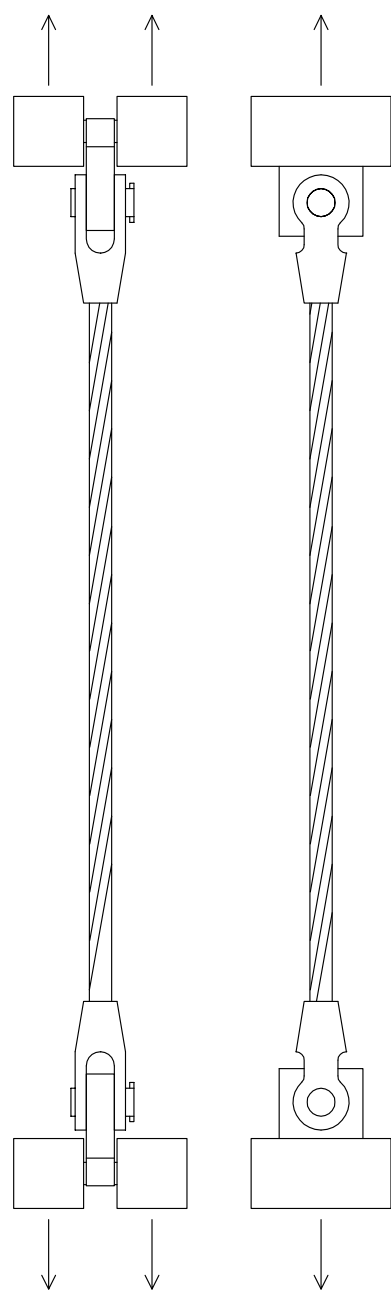


FIGURE B.2: Test set up experiment I

Appendix C

Set up experiment II

In this appendix an overview is given of the equipment used to perform experiment II. Two sets of auxiliary steel plates are required to attach the cables to the tension machine. The design of these plates is also given in this appendix. Figure C.1 shows the two sets of plates used, these plates have a safe working load of 340 kN and 660 kN respectively. In addition to the pad eyes a fork is designed that allows varying diameter pins to be inserted. The cables will be bent over these pins, the fork is shown in figure C.2. Figure C.3 shows the test set up used to perform experiment II.

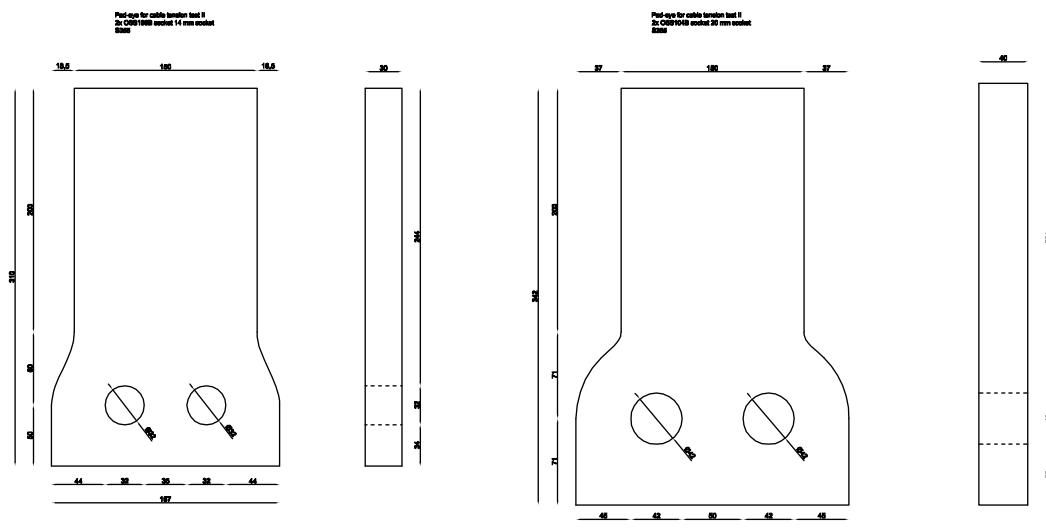


FIGURE C.1: Plates for attaching cables to tensile machine

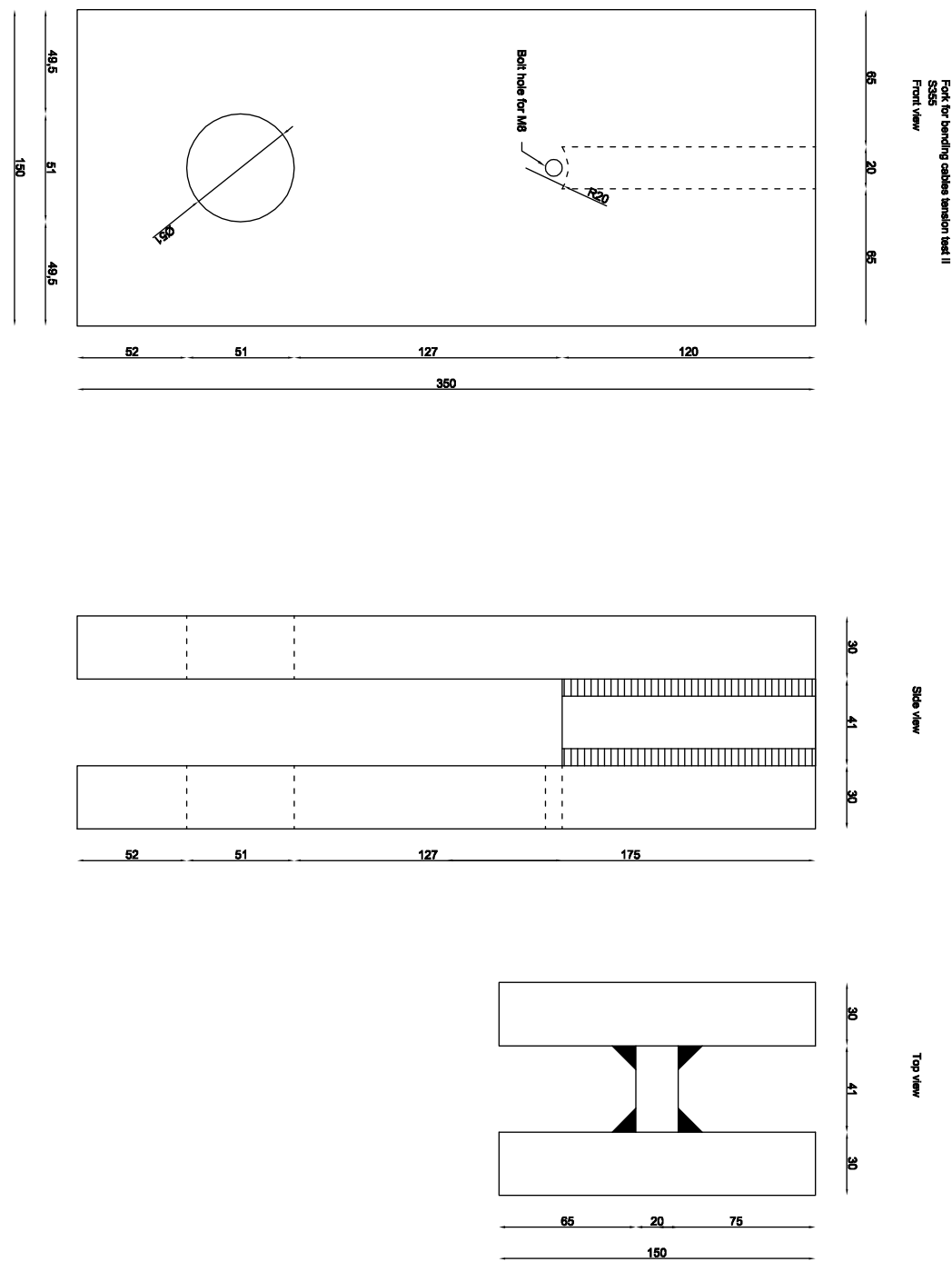


FIGURE C.2: Fork used to bend cables

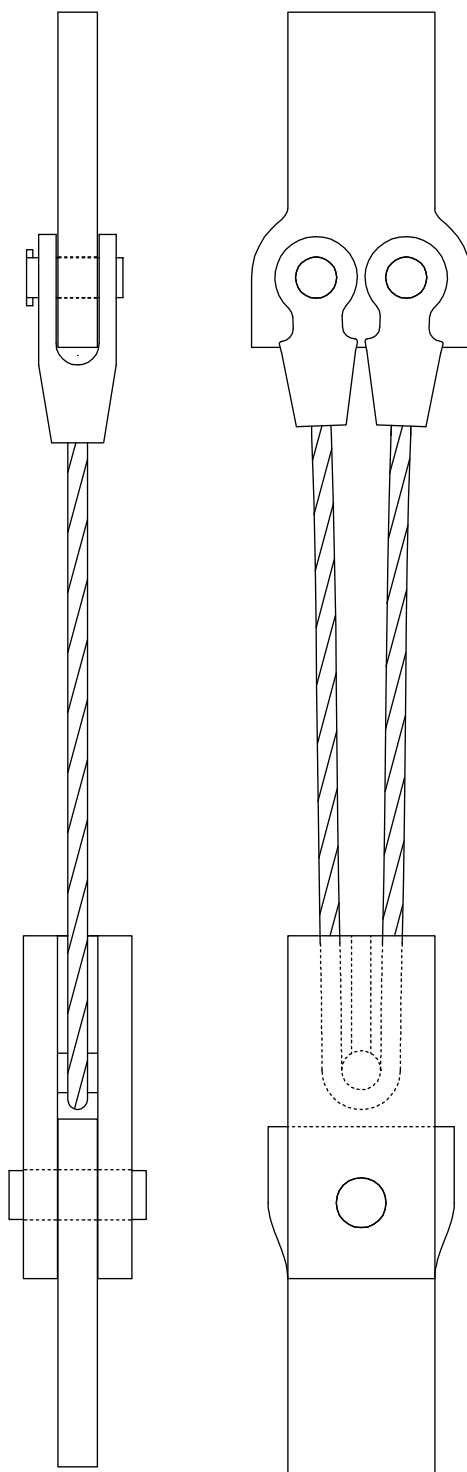


FIGURE C.3: Test set up experiment II

Appendix D

Matlab model

In this appendix the input and output from the Matlab script is elucidated. Especially the input of the geometry of the wire rope requires some additional explanation. Figure D.1 shows what the input looks like in the Matlab script. Most of these parameters should be understandable with the description provided. The input of the geometry however is explained in figure D.2. Figure D.3 shows and explains what the output looks like, where ϕ indicates the wire in an anti clockwise order starting from the neutral axis.

```

%% constants
F_wire_rope=322000;          %[N] axial force
D=21.2;                        %[mm] diameter of the bend
E=196000;                      %[N/mm^2] E-modulus, same for all layers
mu_strands=0.15;               %[-] friction coefficient between wires
mu_wires=0.15;                 %[-] friction coefficient between wires
sigma_ult=1960;                 %[N/mm^2] ultimate strength of steel at 1% strain
e_yield=0.01;                   %strain at yield
e_ult=0.03;                     %strain at break

%wire rope build up
n_strands(1)=1;                %[-] number of strands in layer 1
n_strands(2)=6;                %[-] number of strands in layer 2
n_strands(3)=6;                %[-] number of strands in layer 3
r_strand(1)=0;                  %[-] radius center strand to center of wire rope
r_strand(2)=2.5;                %[-] radius center strand to center of wire rope
r_strand(3)=8.85;               %[-] radius center strand to center of wire rope
laylength_strands(2)=30;        %[mm] lay length of the strand
laylength_strands(3)=80;         %[mm] lay length of the strand

%strand 1 (core)
layers(1)=2;                   %[-] number of layers in strand 1
d(1,1)=0.75;                   %[mm] diameter layer 1
d(2,1)=0.75;                   %[mm] diameter layer 2
d(3,1)=0;                      %[mm] diameter layer 3
d(4,1)=0;                      %[mm] diameter layer 4
laylength_wires(1)=20;          %[mm] lay length of the wires
n(1,1)=1;                      %[-] number of wires in layer 1
n(2,1)=6;                      %[-] number of wires in layer 2
n(3,1)=0;                      %[-] number of wires in layer 3
n(4,1)=0;                      %[-] number of wires in layer 4

```

FIGURE D.1: Input required in Matlab

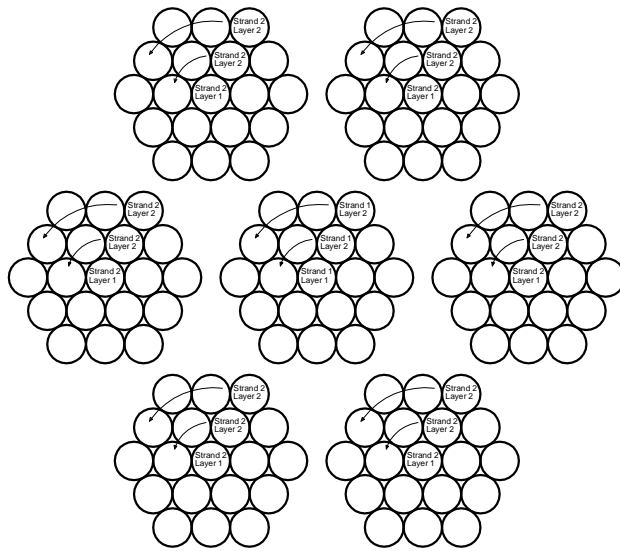


FIGURE D.2: Geometry Matlab input explained

```

Strand 1    reduction_k1 =
              Layer1      Layer2
ψ   0.3307    0.3213
↓
          0       0.3285
          0       0.3285
          0       0.3213
          0       0.3144
          0       0.3144

Strand 2    reduction_k2 =
              Layer1      Layer2
ψ   0.3880    0.3784
↓
          0       0.3873
          0       0.3873
          0       0.3784
          0       0.3698
          0       0.3698

Strand 3    reduction_k3 =
              Layer1      Layer2      Layer3
ψ   0.8020    0.3029    0.7405
↓
          0       0.3267    0.7444
          0       0.3502    0.7483
          0       0.3385    0.7463
          0       0.3148    0.7424
          0       0.2908    0.7386
          0       0.2664    0.7349
          0       0.2541    0.7331
          0       0.2787    0.7368

```

FIGURE D.3: Output given by Matlab

Appendix E

Mathematical derivation strain in wires

In this appendix the difference in strain between a straight wire and a wire in a helix is derived. Figure E.1 shows a straight wire and a wire under the angle β . Under the assumption that the change in lay angle remains close to zero the difference in strain can be expressed according to formula E.1.

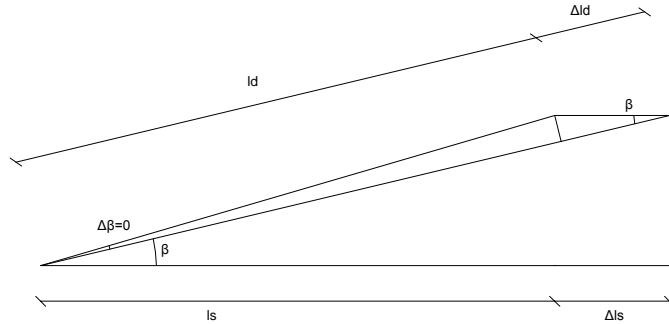


FIGURE E.1: Difference in strain wires between wires due to helix angle

$$\epsilon_d = \frac{\Delta l_d}{l_d}$$

$$\epsilon_s = \frac{\Delta l_s}{l_s}$$

$$l_s = \cos\beta l_d$$

$$l_d = \frac{l_s}{\cos\beta}$$

$$\Delta l_d = \Delta l_s \cos\beta$$

$$\epsilon = \frac{\Delta l_s \cos\beta}{\frac{l_s}{\cos\beta}} = \epsilon_s \cos^2\beta \quad (\text{E.1})$$

Bibliography

- [1] D. Inman K. Spak, G. Agnes. Cable modeling and internal damping developments. *Applied Mechanics Reviews*, 2013.
- [2] K. Papailiou. Bending of helically twisted cables under variable bending stiffness due to internal friction, tensile force and cable curvature. 1995.
- [3] D. Sayenga. History of wire rope. <http://atlantic-cable.com/>, 1999.
- [4] T.K. Caughey H.M. Irvine. The linear theory of free vibrations of a suspended cable. *Proceedings of the royal society*, 1974.
- [5] G. Rega F. Benedettini. Non-linear free vibrations of an elastic cable. *International journal of non-linear mechanics*, 1986.
- [6] B. Schafer P. Hagedorn. On non-linear free vibrations of an elastic cable. *International journal of non-linear mechanics*, 1990.
- [7] G. Costello. *Theory of Wire Rope*. Springer-Verlag, 1990.
- [8] R.E. Hobbs M. Raoof. Analysis of multilayered structural strands. *Journal of engineering mechanics*, 1988.
- [9] A. Cardou C. Jolicoeur. Semicontinuous mathematical model for bending of multi-layered wire strands. *Journal of engineering mechanics*, 1996.
- [10] Y. Chen Y.J. Guan Y.L. Wang L.H. Dai L. Xiang, H.Y. Wang. Modeling of multi-strand wire ropes subjected to axial tension and torsion loads. *International Journal of Solids and Structures*, 2014.
- [11] JX. Wang YH. Sun K. Gao XY. Wang, XB. Meng. Mathematical modeling and geometric analysis for wire rope strands. *Applied Mathematical Modelling*, 2012.
- [12] A. Manes M. Giglio. Life prediction of wire rope subject to axial and bending loads. *Engineering failure analysis*, 2004.
- [13] Union. *Wire Rope User's Handbook*. Springer-Verlag, 2014.

- [14] Det Norske Veritas. *Offshore Standard DNV-OS-H205*. 2014.
- [15] K. Feyrer. *Wire Ropes, Tension, Endurance, Reliability*. Springer-Verlag, 2007.
- [16] G. Fedorko M. Fabian J. Brodniansky S. Kmet, E. Stanova. Experimental investigation and finite element analysis of a four-layered spiral strand bent over a curved support. *Engineering Structures*, 2013.
- [17] B.D. Monelli V. Fontanari, M. Benedetti. Elasto-plastic behavior of a warrington-seale rope: Experimental analysis and finite element modeling. *Engineering Structures*, 2015.
- [18] G. Chen G. Cao Y. Peng, Z. Zhu. Effect of tension on friction coefficient between lining and wire rope with low speed sliding. *Journal of China University of Mining and Technology*, 2007.
- [19] J. Hou S. Fu X. An Y. He.
- [20] Unknown. Strain ageing of steel: Part one. <http://www.totalmateria.com/>, 2013.
- [21] M. Fabian S. Kmet E. Stanova, G. Fedorko. Computer modelling of wire strands and ropes part ii: Finite element-based applications. *Advances in software engineering*, 2011.
- [22] Unknown author. Student's t-test. <http://www.physics.csbsju.edu/stats/t-test.html>, 1999.